Report on model-data comparison and improved model parameterisation

Luis Gustavo Barioni, Gianni Bellocchi, Haythem Ben Touhami, Rich Conant, Jinfeng Chang, Priscilla Pereira Coltri, Abubeker Hassen, Raphaël Martin, Silvia Silvestri, Jason Sicerly, et al.

AnimalChange

SEVENTH FRAMEWORK PROGRAMME

THEME 2: FOOD, AGRICULTURE AND FISHERIES, AND BIOTECHNOLOGIES

Grant agreement number: FP7- 266018

DELIVERABLE 4.4

Deliverable title: Report on model-data comparison and improved model parameterisation

Abstract: The goal of task 4.4 of AnimalChange project is to improve a range of models used to assess climate change impacts on the productivity of pastures, feeding crops and animals.

Due date of deliverable: M36 Actual submission date: M37

Start date of the project: March 1st, 2011 Duration: 48 months

Organisation name of lead contractor: INRA, Gianni Bellocchi

Authors: Luís Gustavo Barioni (EMBRAPA), Gianni Bellocchi (INRA), Haythem Ben Touhami (INRA), Rich Conant (ILRI), Jinfeng Chang (CEA), Priscila Pereira Coltri (CEPAGRI UNICAMP), Abubeker Hassen (UP), Raphaël Martin (INRA), Silvia Silvestri (ILRI), Jason Sicerly (ILRI), Eyob Tesfamariam (UP), Nicolas Viovy (CEA)

Revision: V1

Dissemination level: PU

Table of Contents

1. Executive summary

The report encompasses the experience of AnimalChange consortium in the modelling of crop, grassland and rangeland systems. As the choice of a model type can have an effect on the accuracy of results, there is a need to both understand the properties of different models and reduce uncertainties in the estimates of one or another model over a variety of conditions. In such respect, calibration and evaluation are an essential element of model development and use at a range of scales. The authors present a spectrum of models (and the data that underpin them), for use to assess the impact of climate change at different regions and over different systems. The general objective has been to assemble approaches, applications and prospective developments as a review of the international effort towards the documentation, in a different and much larger scale than today, of impact models of interest for livestock systems. Each chapter is grounded on an extensive bibliography, mostly from international sources but also from national ones (such as thesis in French and Brazilian Portuguese) to broaden awareness of past research results relevant to the project.

An emerging challenge is the upscaling of model estimates, e.g. determination of model parameters for large spatial units. The INRA's experience with the grassland-specific model PaSim is documented, in which advanced techniques (sensitivity analysis and Bayesian statistics) have been applied to identify and calibrate a set of relevant parameters at the European scale. PaSim mechanistic view of grassland carbon and nitrogen fluxes was exploited by CEA to improve ORCHIDEE, a dynamic global vegetation model extensively used in impact studies, which was successfully evaluated in Europe against data of different nature. For both PaSim and ORCHIDEE, the first experiences run by EMBRAPA in Brazilian beef production areas have also been documented, which have opened to the introduction of conceptually important new approaches in view of further testing.

Modelling solutions represent emerging approaches for analyzing climate change impacts in Africa as well. South Africa (UP) provided suitable datasets to assess, in a comparative fashion, a locally-developed model (SWB-SCI) and a flexible tool such as STICS (developed by INRA and mainly evaluated in Europe) for C4 crop and grassland simulations. In Africa, large portions of surface lands are covered by rangelands, complex adaptive systems in which the production of domestic livestock is based on natural or semi-natural plant communities (containing both grasses and woody plants), and where grazing effects are inherently variable and difficult to conceptualise and implement. A contribution to rangeland modelling is given by the experiences gained by ILRI with the model G-Range.

The modelling experiences documented in this report contributed to the understanding of complex agro-ecological systems in different contexts of Europe, South America and Africa. Insights from such experiences will be used in the project to support WP5 activities.

2. Introduction

Crop and grassland ecosystems are complex and dynamic. The many interactions between herbivores, vegetation, soil and the atmosphere, and the role of management practices make our ability to experiment on these systems extraordinarily limited. Thus, testing scenarios of climate change using ecosystem models which simulate physical, chemical, and biological processes in great detail is an imperative. The models that we consider in AnimalChange are deterministic, that is, running the model with the same inputs always produces the same outputs. Using models allows indeed a greater insight and understanding of these processes and interactions than it can be assumed by just considering experimental evidences. They are therefore widely used in climate change impact projections, especially for long-term analyses (Johnson *et al.*, 2008). Such projections need to account for the uncertainty cascade resulting from multiple sources including climate scenarios, the impact model, local climate, vegetation and soil conditions (Olesen *et al.*, 2007; Soussana *et al.*, 2010) and to consider farming practices adaptation (Tubiello *et al.*, 2007).

A major problem with the use of complex ecological models is incomplete incorporation of basic processes in the model structure, as well as input variables and parameter values. This means that model estimates may be affected by a large amount of uncertainties due to uncertainties in parameter values, driving variables (climate, soil and management) and model structure (Gabrielle *et al.*, 2006). There is thus a need of a better match between model outputs and observations (Wallach *et al.*, 2011). At the same time, uncertainty associated with model outputs needs to be quantified and documented (van Oijen and Thomson, 2010).

This report provides an insight on the improvements of the models represented in the AnimalChange consortium, as carried out to better represent plant, soil and atmospheric processes. In particular, it includes:

- Overview of the Pasture Simulation model (PaSim) and applications in Europe (INRA)
- Overview of the Organising Carbon and Hydrology In Dynamic Ecosystems model (ORCHIDEE) and applications in Europe (CEA)
- Developments and applications outside Europe (UP, South Africa; EMBRAPA in collaboration with CEPAGRI UNICAMP, and UFRGS) with models PaSim, ORCHIDEE, STICS and SWB-SCI

3. Improvements in the Pasture Simulation model for applications in Europe

The Pasture Simulation model (PaSim, https://www1.clermont.inra.fr/urep/modeles/pasim.htm) simulates C and N cycling in grassland ecosystems (mixed swards) at a sub-daily time step. The model has evolved over time, starting as a simulator of dry matter production and associated flows of C, N and water in productive pastures (Riedo *et al.*, 1998). It was later improved by Schmid *et al.* (2001) with respect to the production and diffusion of N_2O (Riedo *et al.*, 2002) and the exchange of NH_3 with the atmosphere by Vuichard *et al.* (2007a, b) concerning animal herbage selection and intake, and the effects of diet quality on the emissions of CH_4 from grazing animals. More recently, Graux *et al.* (2011) further improved functionalities to estimate the forage production and dry matter intake taking into account selective grazing between vegetation compartments and the effect of high temperatures, while also simulating ruminants' performance and enteric CH_4 emissions during grazing according to the energetic content of the intake. The livestock system simulates the level of milk and production with heifers, dairy and suckler cows.

The model consists of five interacting modules: microclimate, soil, vegetation, herbivores and management. The soil module simulates soil temperature and moisture profiles based on soil physical properties, hourly weather inputs and simulated plant water use. In the soil module, based on CENTURY soil decomposition approach (Parton, 1988), litter in decomposition over the total soil depth (with no difference between layers) splits into its structural and substrate components, respectively supplying the structural and metabolic soil pools. Other three compartments with different decomposition rates include active, slow and passive pools of soil organic matter. Soil pools are interlinked to represent C and N first-order kinetics. The N cycle considers N inputs to the soil via atmospheric deposition, fertilizer addition, symbiotic fixation by legumes and animal faeces and urine. The inorganic soil N is available for root uptake and is lost through leaching, volatilization and nitrification/denitrification, the latter processes leading to N_2O emissions to the atmosphere. The vegetation module calculates photosynthetic-assimilated C and allocates it dynamically to one-root and three-shoot compartments (each of which consists of four age classes). C losses are through animal milking, enteric CH_4 emissions and returns, and ecosystem respiration. Accumulated aboveground biomass is either cut or grazed, or enters a litter pool. Herbivores are only considered at pasture (not during indoor periods). Management includes organic and mineral N fertilizations, mowing and grazing, setting by the user or optimized by the model.

The improvements introduced to the model thanks to existing partnerships in the frame of AnimalChange are in the follow-up paragraphs, which elaborate on the following points:

1) High-performance computing for climate change impact studies (Vital *et al.*, 2013)
2) Bayesian calibration for European grasslands (Ben Touhami, 2014)

High-performance computing for climate change impact studies

High-performance computing technology permits to efficiently achieve high-performance throughputs for intensive CPU load applications. We developed a pixel-based version of PaSim suited to work with NetCDF format of input and output files. It includes the parallel job launcher, which dispatches individual jobs to execute simulations.

The high-performance computing system was built on the technology already adopted to engineer the dynamic global vegetation model ORCHIDEE (IPSL, 2014), developed with the support of French government-funded research units belonging to the National Institute for Agricultural Research (http://www.inra.fr) and the Alternative Energies and Atomic Energy Commission (http://www.cea.fr). It includes: PaSim grassland model, NetCDF format of data (Network Common Data Form, UNIDATA, 2014), and a job launcher to run executions using Message Passing Interface (MPI) technology to parallel the simulations (Bull, 2014) on a cluster machine (TITANE, CCRT, 2014).
To facilitate coupling with the launcher, version 4.5 of PaSim required the following code modifications: creating the vectored code (*i.e.* able to simulate different pixels at the same time) using only ASCII format input/output files; reading/writing input and output data using NetCDF; restructuring the code into three modules (initialization, main loop and finalization); evoking PaSim modules by the launcher via mixed-programming language using C and Fortran. There is no exchange between the pixels, each pixel being a point and the model running independently for each of the pixels.
In a case study covering metropolitan France (Figure 1), we demonstrate how this approach is configured and used to evaluate the impact of climate change on grassland productivity. Over ~10,000 pixels of 8 × 8 km resolution, we report ~25 h to complete the simulation on the cluster machine TITANE with 200 processors, which is a speedup of 200.

Figure 1. Grassland yield (kg DM m^{-2} yr^{-1}) at 8-km pixel resolution (smoothed images) as estimated for three periods in metropolitan France by downscaled ARPEGE-forced runs of the Pasture Simulation model with the emission scenarios A2.

In the example above, PaSim was inputted with weather and soil data to simulate moderately intensive managed grassland (Table 1) at each pixel.

Table 1. Grassland management used in the model simulations.

Type of grassland	Permanent
Vegetation	Grass mixture
Grazing	Absent
Dates of mowing	May 20, July 1[a], October 5
Nitrogen fertilization	
Date and dose	40 kg ha^{-1}, five days after each cutting
Type of fertilizer	Ammonium nitrate

[a] Optional (under condition of sufficient biomass available).

Weather hourly series were provided for alternative scenarios from 1970 until the end of the 21st century, using ARPEGE climate model downscaled via "weather types" regionalization technique (Boé *et al.*, 2006). INRA InfoSol Unit (Orleans, France, http://www.orleans.inra.fr/orleans_eng/les_unites/us_infosol) supplied soil properties (depth, hydrological properties, pH and texture) split into three soil layers, covering the metropolitan

France with the exception of Paris region (8956 8 × 8 km pixels). For each pixel, soil data were integrated with mean elevation above the sea level and grassland management. Vegetation parameters were taken from published studies (cited by Graux, 2011), while soil carbon pools were set to equilibrium via spin-up runs in the early 1970s (after Lardy *et al.*, 2011).
For each pixel, grassland yields per year were obtained for three 30-year time horizons (extracted from a simulation from 1971 to 2100), representative of near past (1971–2000), near future (2020–2049) and far future (2070–2099). The hourly weather data used to force the model are from the SRES-A2 storyline (IPCC, 2000), corresponding on average to concentrations of atmospheric CO_2 for the three time slices of 346, 462, and 717 ppmv, respectively. Outputs, including gross and net primary productivities, carbon fluxes and yield were aggregated into annual averages and displayed for map viewing. The result of the pixel-based rendering is displayed in the dry matter (DM) yield maps of Figure 1, as generated by using Panoply Data Viewer (DataONE, 2014), set to read and process NetCDF output files. These illustrative results reflect potentially different patterns in relation to climate change (increased risks in the near future for grassland productivity near the Mediterranean coast, opportunity for greater productions in inland areas of France) as also suggested by the French National Observatory for the Effects of Global Warming (http://www.onerc.org) but viewed with major detail and graphical resolution.

Bayesian calibration for European grasslands

Using the principle of Bayesian calibration (Ben Touhami *et al.* (2013b), PaSim was used to update prior parameter distribution to achieve a posterior distribution (30000 iterations with acceptance rate of about 30%) by incorporating the information contained in the measured data of seven multi-year observational grassland sites in Europe (Amplero, Italy; Bugac-Puszta, Hungary; Easter-Bush, United Kingdom; Früebüel and Oensingen, Switzerland; Laqueuille intensive and extensive plots, France) mainly derived from the FLUXNET network (http://fluxnet.ornl.gov).

The nine most relevant PaSim vegetation parameters (chosen from Europe-wide sensitivity analysis, Ben Touhami *et al.*, 2013a) were calibrated using a set of soil (temperature, water content), vegetation (leaf area index, harvested biomass) and atmospheric (NEE) measured variables. The calibrated model was used to assess CO_2 (NEE, g C m^{-2} d^{-1}) and CH_4 (g CH_4-C m^{-2} d^{-1}) fluxes based on the eddy covariance measurements (in place since 2002) of Laqueuille in France (45° 38' N, 02° 44' E, 1040 m a.s.l.). Two paddocks were continuously grazed by heifers from May to October with two management options (Klumpp *et al.*, 2011): the intensive management paddock included significant amounts of N fertilization (three times per year for a total of ~200 kg N ha^{-1}) and annual average stocking rate of 1.1 LSU ha^{-1}; the extensive management paddock had no fertilization and 0.6 LSU ha^{-1}.

The improvement of simulation after parameters calibration is reflected in the posterior estimates (thanks to maximum likelihood) of NEE and CH_4 daily values, which are closer to observations than using the prior distribution. For NEE from multiple years (2004-2008), regression lines (Figure 2) show the improvement obtained with posterior parameter values (higher R^2; slope and intercept closer to 1 and 0, respectively), with no difference between managements. Daily CH_4 observed values were limited to May-October 2010 in the intensive system.

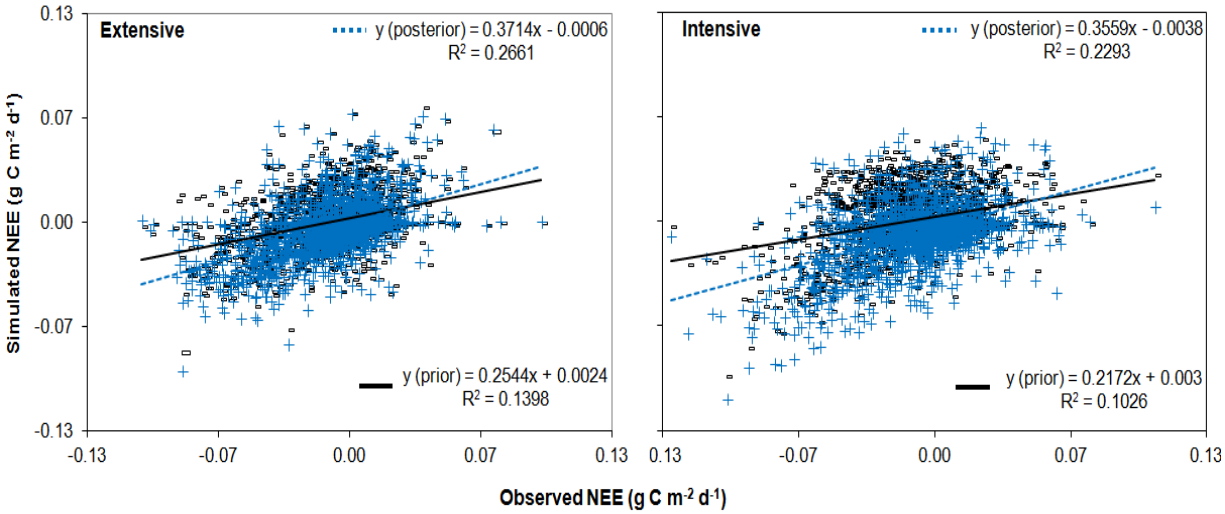

Figure 2. Scatterplots of simulated (prior [-] and posterior [+]) and observed NEE values (g C m^{-2} d^{-1}) at ther French site of Laqueuille (2004-2008), with regression lines for extensive and intensive management (posterior estimates were obtained under the hypothesis of uniform distribution of parameter values within a given range).

Figure 3 shows the improvement obtained with the posterior parameterization but also that the model is not properly simulating the fluctuation in CH_4 values. It is noteworthy that, with posterior simulation, the system emits enteric CH_4 fluxes in summer because enough grass biomass is available and grazing may occur. This approximates what happens in reality, which is not the case with prior parameterization.

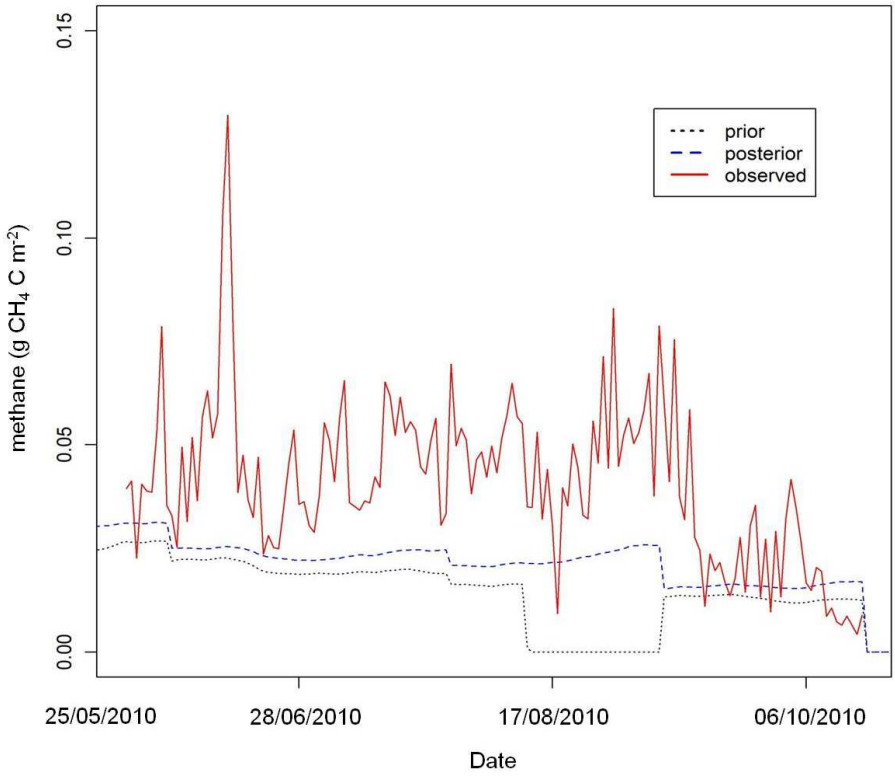

Figure 3. Simulated (prior and posterior) and observed CH_4 values (g C m^{-2} d^{-1}) at the French site of Laqueuille (intensive management) over May-October 2010 (posterior estimates were obtained under the hypothesis of uniform distribution of parameter values within a given range).

Table 2 summarizes, for four output variables, the performances of PaSim at four sites not included in the calibration exercise. Two performance indices were used:

$$\mathrm{RMSE} = \left[\frac{\sum_{i=1}^{n}(P_i - O_i)^2}{n}\right]^{0.5}$$

$$\mathrm{CRM} = \frac{\sum_{i=1}^{n}(O_i - P_i)}{\sum_{i=1}^{n}(O_i)}$$

The root mean square error (RMSE), varying between 0 (best) and positive infinity, quantify the amount of departures of estimates (*P*) from observations (*O*). The coefficient of residual mass (CRM) may range from negative to positive infinity, where negative values indicate over-estimation and vice versa (0 being the optimum).

Table 2. Evaluation of priori and posterior estimation of four output variables (all validation sites confounded). Posterior estimates were obtained under two hypothesis of distribution of parameter values. RMSE: root mean square error; CEM: coefficient of residual mass.

Distribution	Information	Soil water content (%)		NEE (g C m^{-2} d^{-1})		GPP (g C m^{-2} d^{-1})		Aboveground biomass (g DM m^{-2})	
		RMSE	CRM	RMSE	CRM	RMSE	CRM	RMSE	CRM
Uniform	**Prior**	0.12	0.09	0.02	-1.21	0.35	0.04	15.76	0.39
	Posterior	0.12	0.08	0.02	0.76	0.34	0.02	15.13	0.33
Gaussian	**Prior**	0.13	0.10	0.02	-1.21	0.34	0.05	17.28	0.44
	Posterior	0.13	0.09	0.02	0.76	0.30	0.01	16.24	0.40

Globally, these results (and others not shown, Ben Touhami and Bellocchi, 2014) indicate that the parameterization of PaSim obtained via Bayesian calibration at multiple European sites has improved simulation of a variety of output variables, though without compensating for limitations in the model structure. This means that the modelling of C exchanges and GHG fluxes from grasslands in Europe merits further investigation. This is a non-trivial task, not only because of unsolved theoretical questions but also because fluxes are affected by large observational uncertainties.

Conclusions

The pixel-based software for grassland simulations provides the power of the high-performance computing with simplicity and flexibility for configurable applications dedicated to climate change impact studies. The pixel-based version of PaSim is sufficiently stable to perform projections of impact. However, the user needs to know the technical details (knowledge of the used cluster environment) about the job submission related to the system environment setup and the developed code is tightly coupled to its application. These are issues for future work, which translate into the need of supporting various platforms and applications, and automating a vast array of processes, as addressed through modern approaches to job scheduling and workload automation solutions. The new capabilities hold promise for modellers to widen the scope of climate change impacts on grasslands, yet at high resolution of local topography and weather features. Moreover, the tool for pixel-based, mechanistic simulation of grasslands (with biogeochemical capabilities) is a general way to facing climate change impact studies while capturing complex multi-scale issues. Given the dearth of methods that integrate the presentation of spatially refined gridded maps with

uncertainty together, it may support the communication flow of the impacts and the co-construction of knowledge among scientists and stakeholders. The use of advanced statistical approaches (such as Bayesian calibration) opens to the opportunity of reducing uncertainties when using upscaled parameter values.

4. Development and validation of the ORCHIDEE Grassland Management module ORCHIDEE-GM

Introduction

ORCHIDEE is a process-driven dynamic global vegetation model (DGVM) designed to simulate C and water cycle from site-level to global scale (Ciais *et al.*, 2005; Krinner *et al.*, 2005; Piao *et al.*, 2007). It is composed of two main modules. The SECHIBA (soil–vegetation system and the atmosphere) parameterization computes the energy and hydrology budget on a half-hourly basis, together with photosynthesis based on enzyme kinetics (Viovy and de Noblet, 1997). These results are fed into a module of ORCHIDEE called STOMATE, which simulates C dynamics on a daily basis: gross primary production (GPP) is allocated to different organs, and then respired by the plant or by soil microorganisms when parts of the plant die. These processes determine several ecosystem state variables such as leaf area index (LAI) and canopy roughness, which are fed back into SECHIBA because they control the energy and water budgets. The equations of ORCHIDEE are described in Ducoudré *et al.* (1993) for SECHIBA and in Krinner *et al.* (2005) for STOMATE, and can be found at http://orchidee.ipsl.jussieu.fr. As in most DGVMs, the vegetation is discretized into a discrete number (13) of PFTs over the globe. For grassland, C3 and C4 grass are included and treated like unmanaged natural systems, where C–water fluxes are only subject to atmospheric CO_2 and climate changes. Here we use version 1.9.6, which can be accessed at http://forge.ipsl.jussieu.fr/orchidee/browser/tags/ORCHIDEE_1_9_6. The N cycle is not included in this version of ORCHIDEE.

PaSim is a plot-scale process-based grassland model developed by Riedo *et al.* (1998), which simulates grassland processes at a sub-daily time step. It considers a soil–vegetation–animal atmosphere system (with state variables expressed per m^2) and runs over one to several years. PaSim allows simulating main grassland services such as forage and milk production, as well as the C, N, water and energy fluxes in sown and permanent grasslands. PaSim was applied on a grid to make simulations of grasslands GHG fluxes at the European scale by Vuichard *et al.* (2007b) and was used to run an ensemble of climate change impacts simulations on grassland services and GHG budgets at French sites (Graux *et al.*, 2012, 2013). PaSim comprises six modules, simulating plant growth, microclimate, soil biology, soil physics, animal processes, as well as management options. The two latter modules use a daily time step, just as STOMATE does in ORCHIDEE. See Graux *et al.* (2012, 2013) for further details about the modelling of grassland processes.

Model developments

Coupling strategy

To incorporate into ORCHIDEE a description of management, our approach is to take the cutting, grazing and fertilization options, and the animal module of PaSim (version 5.0, see above) and integrate them into ORCHIDEE. Each day, ORCHIDEE provides AGB to the management module to be used for cutting or grazing (Figure 1).

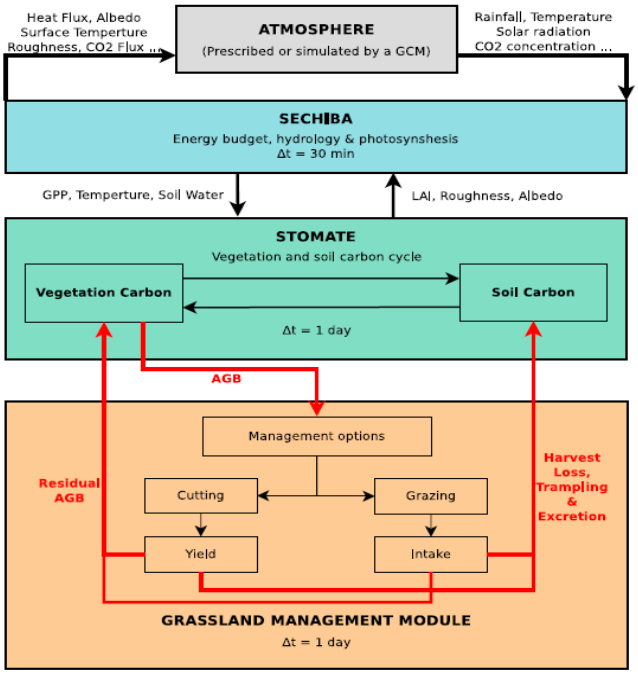

Figure 1. Schematic view of ORCHIDEE-GM.

Taking into account the types of herbivores (different types of cattle or sheep), the management module simulates harvested biomass, herbage intake and animal trampling during grazing, and following C fluxes by animal respiration, milk production, CH_4 emissions, and excreta returns. Then it feeds back two variables into ORCHIDEE, the residual AGB fraction, and the newly formed litter. The litter pool of ORCHIDEE is modified from the input of harvested grass residues, manure additions, and from animal trampling effect and excreta returns. We will hereafter refer to the modified version of ORCHIDEE as ORCHIDEE-GM (grassland management). Nine parameters are required for the simulations: (i) the timing of cuts and the associated residual total shoot DM(and the residual LAI), (ii) the type of fertilizer, the timing of their application and the corresponding amounts, and (iii) the start and length of grazing periods and the grazing animals stocking rate.

Specific modifications in the ORCHIDEE-GM

As ORCHIDEE is designed to represent the C cycle of unmanaged grassland, we adapted the model to include (i) the possibility of reaching high LAI values such as observed in productive managed European grasslands; (ii) the leaf shed in highly dense tillers; (iii) a reduction of the leaf fraction in total AGB, and iv) a translocation of carbon from a reserve pool after cut in order to shape new leaves. In addition, we improved the representation of specific leaf area (SLA) for stimulating regrowth after cutting or grazing.

Evaluation at European grassland sites

Site selection and description

To evaluate ORCHIDEE-GM, we ran ORCHIDEE and ORCHIDEE-GM at 11 European grassland sites with contrasted management intensity, where good quality flux data (NEE,

measurements by eddy-covariance (EC) technique) were collected, the data being gap-filled and partitioned to GPP and TER (total ecosystem respiration) using the CarboEurope-IP methodology (see CarboEurope-IP project, *e.g.*, Dolman *et al.*, 2006; Reichstein *et al.*, 2005; Papale *et al.*, 2006; Moffat *et al.*, 2007; Béziat *et al.*, 2009). The 11 sites have sufficiently detailed management records (management type, timing of cutting or grazing, and correspondingly harvest severity or stocking density). There are three cut sites, six grazed sites and two mix-managed sites. The geographic information, management type, fertilization practice, year with management or C fluxes records, and mean meteorological data.

Site-level simulations were conducted with ORCHIDEE and with ORCHIDEE-GM separately. All simulations started from an equilibrium state of C pools with climate and management obtained with a model spin-up and additional 40-year simulations after spin-up were done to obtain the ecosystem C pools under the grassland management. Finally, starting from the end of spin-up 2, simulations were conducted for the target period of evaluation.

Methods for evaluating model performance

To assess model–data agreement for biometric variables such as LAI and AGB, we use the index of agreement (IOA, Willmott *et al.*, 1985; Legates and McCabe, 1999). Ecosystem–atmosphere fluxes are shaped by a variety of fluctuations on different scales of characteristic variability. Scalar error estimates and residual analysis used to summarizing model–data disagreement provide only limited insight into the quality of a model (Mahecha *et al.*, 2010). A more sophisticated way could be localizing model–data mismatches in time (Gulden *et al.*, 2008). Thus, to evaluate time-frequency localized model performance on CO_2 fluxes (GPP, TER and NEE), we used a time domain decomposition method called SSA (singular-spectrum analysis; Broomhead and King, 1986; Elsner and Tsonis, 1996; Golyandina *et al.*, 2001; Ghil *et al.*, 2002).

Model performance for CO_2 fluxes

ORCHIDEE-GM reproduces intra-annual fluctuations of CO_2 fluxes significantly affected by grassland management, either cut (Figure 2) or grazed.

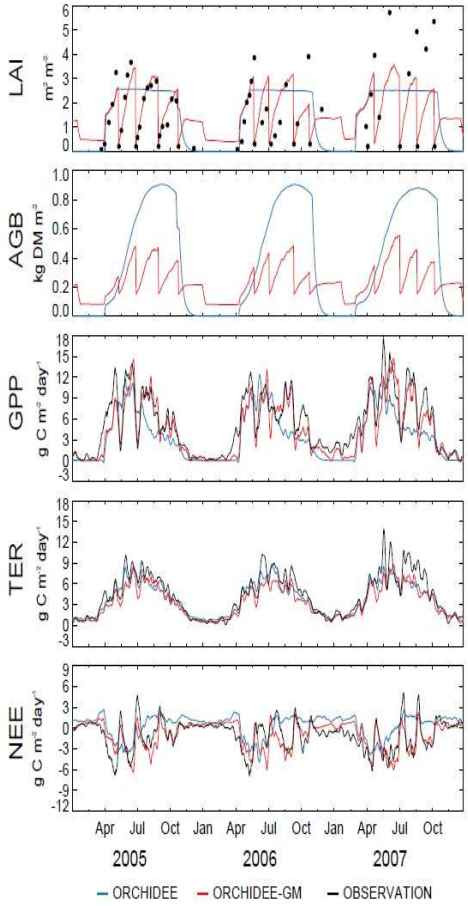

Figure 2. Simulations at Oensingen (Switzerland).

A better model performance in ORCHIDEE-GM compared to ORCHIDEE on intermonthly and seasonal–annual scales is found for NEE and GPP. This further justifies the necessity to incorporate management processes in order to calculate the CO_2 exchange on European grasslands, *e.g.*, for being used as a better prior of atmospheric CO_2 inversions. In addition, an increase in the ability to reproduce NEE at timescales of weeks to year can be attributed to a better simulation of GPP rather than TER that improves marginally. This might be due to the modelling issue of soil organic matter initial disequilibrium (Carvalhais *et al.*, 2008). Improved GPP simulation by ORCHIDEE-GM comes from more accurate prediction of plant growth under management. However, the main component of TER is soil respiration. It is highly sensitive to soil organic matter amount, which is initialized by the same soil C module in ORCHIDEE rather than by field observations in this study. Although ORCHIDEE-GM performs better on both timescales, systematically better at cut sites than at grazed sites, the improvement at grazed sites are more noticeable on the seasonal–annual than on the intermonthly timescales. This illustrates the fact that cut and grazing practices have different influences in the temporal variation of NEE, and that grazing has more impact on seasonal–annual than on intermonthly timescales. The large amplitude on intermonthly timescale indicates that the intense sporadic disturbance, *e.g.*, cut, could also significantly influence CO_2 fluxes. Figure 3 summarize the improvement of RMSE with ORCHIDEE-GM for the 11 sites.

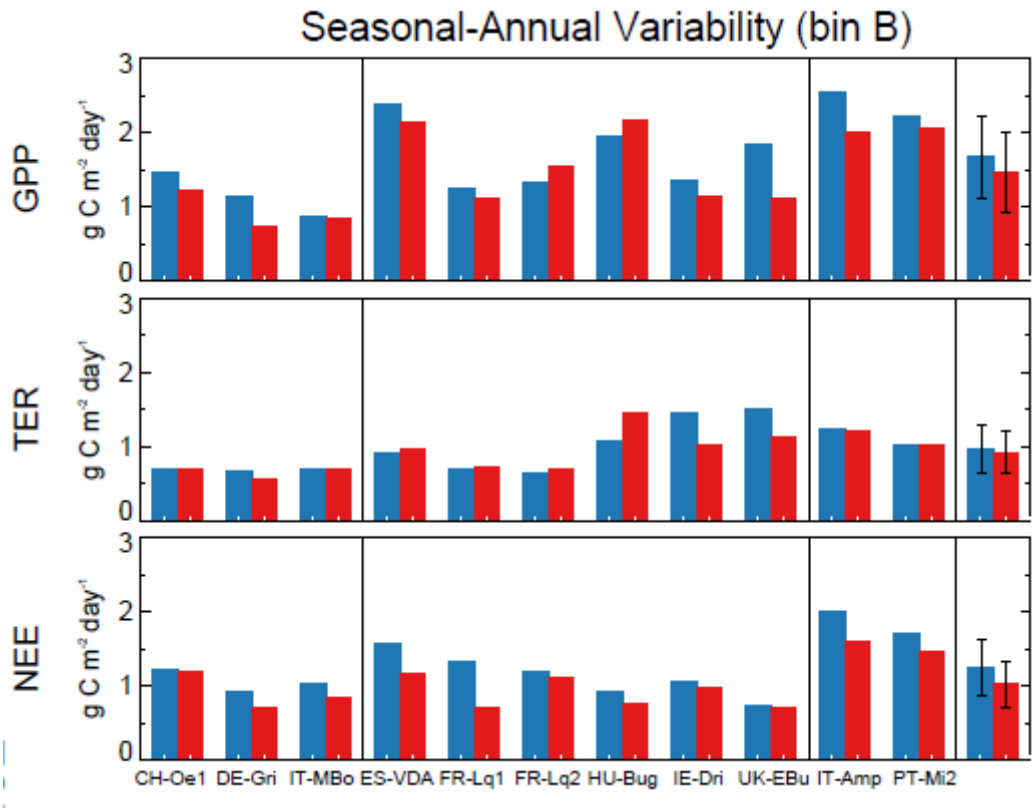

Figure 3. RMSE for three CO_2 fluxes (blue: ORCHIDEE; red: ORCHIDEE-GM).

Validation at European scale

The optimal animal stocking rate, S_{opt} (number of livestock units (LSU) per hectare) and the optimal proportion of grazed versus cut grasslands, F_{opt} (within [0, 1]) are calculated for each grid cell using the optimization algorithm of Vuichard *et al.* (2007a). The annual herbage production, *Y*, (kg of dry matter (DM) per hectare) of cut grasslands that occupy a fraction ($1-F_{opt}$) of a grid cell should be equal to the herbage dry matter required by herbivores under cover, *X* (kg DM ha^{-1}) during the non-growing season, when grazing is not possible. This rule is expressed as a system of two equations with two unknowns (*X* and F_{opt}):

$$X = Y'(1 - F_{opt}) \quad (1)$$

$$X = IC \times \Delta T_{farm} \times S_{opt} \times F_{opt} \quad (2)$$

where *IC* is the daily intake capacity (with a default value of 13 kg DM LSU^{-1} day^{-1}; IPCC, 2006) of animals under cover, ΔT_{farm} is the number of non-growing season days during which herbivores need to be fed with cut herbage. The potential animal density (D_{opt}) is given by:

$$D_{opt} = S_{opt}'F_{opt} \quad (3)$$

D_{opt} is calculated in the iterative algorithm by increasing the input animal stocking rate (S_{opt}) until convergence is reached and the stocking rate reaches its potential value and cannot increase further. D_{opt} must be interpreted as a potential herbage-only limited livestock density of a given model grid cell (similar to the term "livestock carrying capacity", IUCN/UNEP/WWF, 1991). When D_{opt} is reached, the grassland herbage production is fully used by livestock and the herbage intake capacity of the livestock is reached.

Modelling adaptive management in response to climate variability and CO_2

We *t* defined new rules that were incorporated into ORCHIDEE-GM to account for how grassland management might change in response to a climate-driven change in productivity. We start from animal stocking rate (S_{opt}) and proportion of grazed grasslands (F_{opt}) optimized for a given productivity (in equilibrium with climate). If productivity then changes (because of climate change), we assume that farmers will take adaptive actions to restore the biological potential livestock density by changing livestock numbers. Specifically, at the end of a given year, *i*, the farm manager in each grid cell takes the decision to add (in case of forage surplus) or to remove (in case of forage deficit) animals to or from the grid cell for the next year, thus changing the previous optimal animal density ($D_{opt,i}$) by a step $\Delta D_{opt,i}$ as function of the forage surplus or deficit (M_i). The new optimal animal density for the next year *i+1* ($D_{opt,i+1}$) is given by:

$$D_{opt_{i+1}} = D_{opt_i} + DD_{opt_i} \quad (4)$$

where $D_{opt,i+1}$ is adapted in the model by changing F_{opt} (in Eq. 3), and the step density change ($\Delta D_{opt,i}$) is given by:

$$DD_{opt_i} = DD_{opt}{}'\alpha = M_i\, IC/DT_{year}{}'\alpha \quad (5)$$

where *IC* is the daily intake capacity, ΔT_{year} = 365 days. ΔD_{opt} is the maximum animal density change resulting from the forage surplus (or deficit) of the previous year (M_i), and α is the fraction of ΔD_{opt} that is realized by the farmer. The value of α is adjustable, and we chose 20% here, representative of a "moderate risk tolerance" decision by the farmer to changing animal density to adapt to the new productivity conditions. Hence, M_i is given by:

$$M_i = X'_i - X_i \quad (6)$$

where, in each grid cell, X'_i is the annual total grass production from cut grasslands for the year *i*, calculated from Eq. 1, and X_i is the herbage dry matter required by herbivores under cover during the non-growing season for the year *i*, calculated from Eq. 2.

ORCHIDEE-GM is integrated on a grid over Europe using the harmonized climate forcing data from the ERA-WATCH reanalysis for the period 1901–2010 and at a spatial resolution of 25' by 25'. The climate variables were simulated by REMO regional climate model (http://www.remo-rcm.de) and harmonized using WATCH forcing data methodology (Weedon *et al.*, 2010, 2011). This resolution is sufficient to represent regional meteorological regimes accurately in low lying regions, but not in mountainous areas. Gridded nitrogen fertilizer application rate for European grasslands (at a spatial resolution of 25' by 25'; including mineral and organic fertilizer) was estimated and spatial dis-aggregated by CAPRI model (see Leip *et al.*, 2008 for details of the method) based on regional and national statistics (*e.g.* AGRESTE statistics and Eurostat). Some countries were ignored due to the missing or too bad quality of statistical data (*e.g.* Switzerland and Norway). Three levels of nitrogen-addition intensity (low, medium and high intensity) were provided for the year 2010. A set of rules was used to rebuild the temporal evolution of gridded nitrogen fertilization: 1) only organic fertilizer was applied with low intensity during the period 1901–1950; 2) mineral fertilizer was applied since 1951; 3) from 1951 to 2010, the application rate of both mineral and organic fertilizer were linearly evolved from level of low intensity (for the year 1951) to level of medium intensity (for the year 2010).

A series of simulations was carried out. ORCHIDEE-GM was first run for a spin-up (simulation E1) without management using the first 10 years of climatology data (1901–1910) recycled in a loop, and the atmospheric CO_2 concentration for 1900 (296 ppm) until the carbon pools reached equilibrium (long term Net Ecosystem Exchange, NEE = 0 at each grid

point). This first spin-up usually takes 10,000 years. Starting from the end of this first spin-up, two separate transient simulations were performed. In the first one (simulation E2), optimal animal stocking rates (S_{opt}) and fractions of grazed grassland (F_{opt}) for the period 1901–1910 were defined by running ORCHIDEE-GM with its optimization algorithm that maximizes stocking rates in each grid cell (see above and Vuichard *et al.* 2007a). In the simulation E3, ORCHIDEE-GM was run during the historical period (1910–1960) with increasing atmospheric CO_2, variable climate, and with the new adaptive management change algorithm. This simulation started with the reference distributions of S_{opt} and F_{opt} over Europe (obtained in simulation E2), as well as with soil carbon pools for the year 1910 (end of the spin-up simulation). Starting from the end of simulation E3, formal simulation E4 was carried out for the period 1961–2010 with increasing atmospheric CO_2, variable climate, and with the adaptive management change algorithm. Three further simulations (E5, E6 and E7) investigated the relative contribution of atmospheric CO_2, climate change and nitrogen fertilization trends on the estimated trend in productivity. The simulations E5, E6 and E7 are the same as simulation E4, but with atmospheric CO_2 concentration fixed at the level of 1961 (E5), using the first five years of climatology data (1961–1965) recycled (E6), or with nitrogen fertilization fixed to the level of 1961 (E7), respectively. The difference in productivity trend between simulations E3 and E4 reflects the effects of increased CO_2. The effects of climate variation and nitrogen fertilization were derived as the difference between simulations E3 and E5 and between simulations E3 and E6, respectively.

Data for evaluating the simulated productivity of European grasslands

Smit et al. (2008) constructed a map of Europe showing the spatial distribution of grassland productivity by integrating census statistics, literature, and expert judgment using the NUTS classification (Eurostat, 2007). The biological potential of grassland productivity from ORCHIDEE-GM (on a spatial resolution of 25') was aggregated to the NUTS-2 level weighted by the corresponding grassland area in each grid cell (from CORINE Land Cover map, CLC2000; Büttner et al., 2004). We then compared the spatial pattern of modelled potential productivity with the map by Smit et al. (2008) averaged over the period 1995–2004.

Livestock distribution and its ratio to productivity

FAO (Wint and Robinson, 2007) provides a 5' by 5' global livestock distribution maps for major animal species (cows, pigs, poultry, sheep, goats, and buffalo), which are consistent with regional statistics. Cattle, sheep and goat densities are expressed in this study as the number of animals (head) per square kilometer of land suitable for livestock production (Wint and Robinson, 2007). A ruminant livestock density in LSU ha^{-1} was calculated from these data by using head-to-LSU conversion factors of 0.8, 0.1, and 0.1 for cattle, sheep and goats, respectively. This LSU density distribution was then aggregated to the 25' by 25' grid used by ORCHIDEE-GM. We also aggregated the livestock density distribution from FAO to the NUTS-2 level, for comparison with grassland productivity statistics from Eurostat summarized by Smit *et al.* (2008). Then, the average ratio of FAO livestock density to grassland productivity from the Eurostat data was calculated in each NUTS region.

Grass-fed livestock numbers estimated from statistics and model simulations

In Europe, ruminant livestock are not only fed on grass, but also receive arable crop-feed and crop by-products. Thus, the number (LSU) of grass-fed livestock (N_{obs}) in each region

can be calculated separately as:

$$N_{obs} = N_{beef}{}'F_{beef} + N_{dairy}{}'F_{dairy} + N_{sheep}{}'F_{sheep} + N_{goats}{}'F_{goats} \quad (7)$$

where N_{beef}, N_{dairy}, N_{sheep} and N_{goats} are the numbers (LSU) of beef cattle, dairy cattle, sheep, and goats calculated from regional census statistics; F_{beef}, F_{dairy}, F_{sheep} and F_{goats} are the fractions of grass-feed in the diet of each type of animal available from the study by Wirsenius (2000) (Western and Eastern Europe).

ORCHIDEE-GM simulates the biological potential livestock density D_{opt} on a 25 km grid over Europe. This model output was re-aggregated to the NUTS level (D_{reg}, for NUTS-0 to NUTS-2) and weighted by the actual grassland area of each grid cell from CORINE Land Cover map (*CLC2000*). The simulated grass-fed livestock (N_{sim}) is given by:

$$N_{sim} = f_{temp}{}'D_{reg}{}'A_{temp} + f_{perm}{}'D_{reg}{}'A_{perm} + f_{rough}{}'D_{reg}{}'A_{rough} \quad (8)$$

where A_{temp}, A_{perm}, and A_{rough} are the area of *temporary grassland*, *permanent grassland*, and *rough grazing* respectively in each NUTS region (data from Eurostat; names in italics from Eurostat terminology, see above); f_{temp}, f_{perm}, and f_{rough} are the fraction of D_{reg} that grassland of different types are assumed to support, and are set to 100%, 80%, and 10% for temporary grasslands, permanent grasslands, and rough grazing lands respectively according to their productivity. Newly sown temporary grassland has high productivity, and thus is assumed to support the simulated potential stocking rate, whereas less productive *rough grazing* grasslands are assumed to receive little management and to support only 10% of D_{reg} (these grasslands are usually located in mountainous areas with steep slopes and limited accessibility). Combining modelled livestock density with statistical grassland-area data, we produced a simulated number of animals for each region, N_{sim} that can be compared with N_{obs} available from the statistics.

Unfortunately, long-term regional time series of grassland area and livestock numbers (N_{obs}) are not available for the Eurostat NUTS regions. Therefore, country averages N_{obs} (also called NUTS-0) from 30 countries from the FAO statistical database (FAOstat) were used to evaluate modelled trends of N_{sim} over the period from 1961 to 2009.

Evaluation of grass-fed livestock numbers in Europe

Regressing the simulated numbers of grass-fed animals (N_{sim} in Eq. 8) against the Eurostat data (N_{obs} in Eq. 7), gives a (spatial) coefficient of determination $R^2 = 0.88$ ($P < 0.01$) for the NUTS-2 regions (slope = 0.98; NUTS-1 for Germany). Country scale (NUTS-0) comparison (Figure 4) shows the mean value and standard deviation of the observed and modelled grass-fed livestock numbers during the period 1990–2010. When the comparison is made for regions grouped into Köppen-Geiger climate zones N_{sim} is comparable to N_{obs} in regions with moist temperate climate (climate zones Df and Cf, with cold winters and mild winters respectively; slope close to 1, $R^2 > 0.7$, $P < 0.0$). However, ORCHIDEE-GM tends to underestimate the number of grass-fed livestock in regions with high latitude climate (zone ET, *e.g.*, Norway) and in Mediterranean countries (zone Cs, *e.g.*, Greece, Italy, Spain and Portugal).

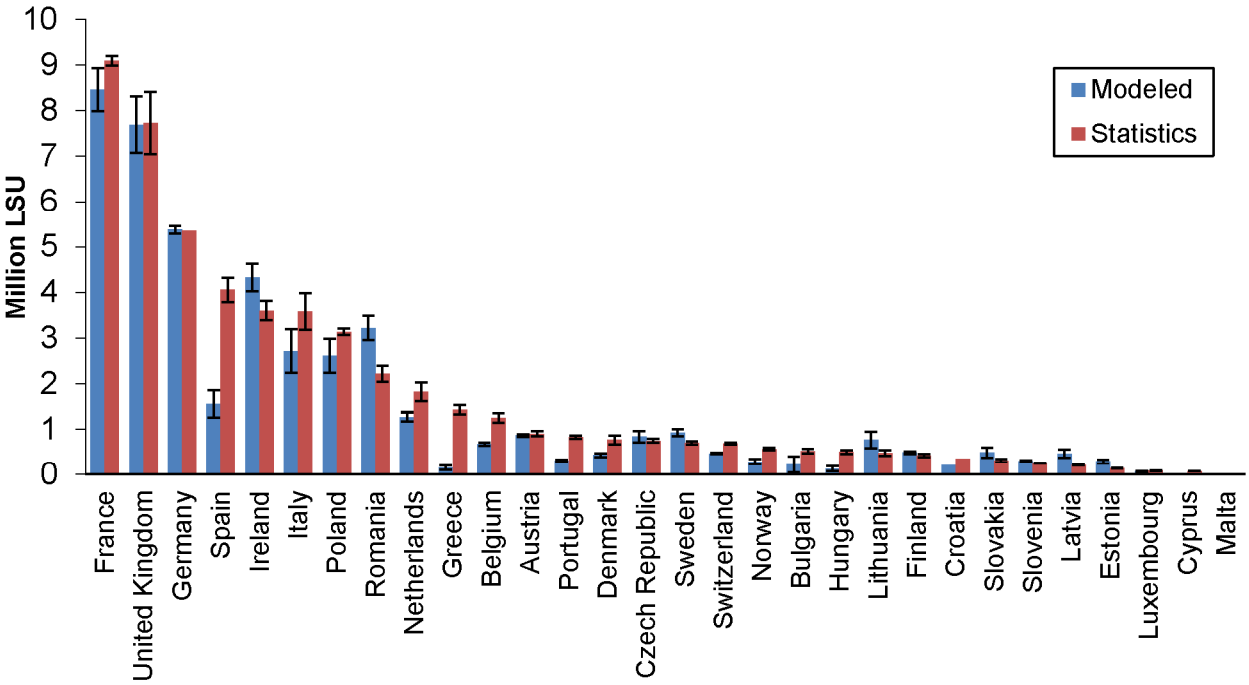

Figure 4. Comparison of modelled and observed (Eurostat) grass-fed livestock numbers by NUTS-0 level (countries) for the period 1990-2010.

Decadal trends and interannual variability of grassland productivity

Figure 5 shows the decadal trend of simulated grassland productivity compared to statistics. For European grasslands, ORCHIDEE-GM estimates a small average annual increase of potential productivity over the last five decades (0.30% per year) which reflects the effects of elevated CO_2, climate change and nitrogen fertilization. Changes in other drivers such as nitrogen deposition and other management drivers (except nitrogen fertilization) in this period are not included in the model because the data (*e.g.*, nitrogen deposition) are not available over this period (1961–2010). Meta-analyses revealed that nitrogen fertilization itself could stimulate grass biomass by around 50% (Le Bauer and Treseder, 2008; Xia and Wan, 2008), and the positive biomass responses could be significantly enhanced when CO_2 enrichment and/or the addition of other nutrients (such as phosphorus) were taken into account (Elser *et al.*, 2007; Xia and Wan, 2008). Such a strong effect of fertilization, however, was neither observed in regional-scale productivity statistics, nor in modelled potential productivity. We believe there are two reasons for this lack of response: i) Intensive fertilization that would strongly improve productivity, has not been fully applied to all grasslands in Europe (a large part of the total grassland area was fertilized with only 0-40 kg N ha^{-1} yr^{-1}). ii) Fertilization and the improvement of grass species by plant breeding were introduced only a few decades ago in sown (*i.e.* temporary) grasslands, and with apparently limited effects on productivity. On the other hand, it has been shown that water stress is a major limitation on grassland productivity (Le Houerou *et al.*, 1988; Knapp *et al.*, 2001; Nippert *et al.*, 2006) and a few grasslands are irrigated in Europe (Wriedt *et al.*, 2009). Thus, in contrast to arable agriculture (annual crops), grasslands, which are still largely semi-natural in Europe, display changes in productivity over recent decades that are primarily controlled by climatic and atmospheric factors and not by management.

Land-use change could be another significant and non-modelled factor that impacts the long-term trends of grassland productivity in some EU countries. Transition to arable crops and abandonment can both mark a land-use change affecting grasslands. For example, in the

Czech Republic, besides the impact of unfavorable climate factors captured by our model, grasslands were also abandoned during the transition to a market economy, causing a sharp drop in productivity. In Italy, the evolution of grassland productivity has also been impacted by major land-use changes. The number of grazing animals has decreased owing to the abandonment of low-productive dry rangelands (Peeters, 2009). At the same time, grassland areas with favorable conditions have been partly converted to fodder maize and to cash crops (Peeters, 2009).

In certain regions, changes in the management of grasslands, such as fertilization, may have reduced the variability of productivity between years. However, significant interannual variability of grassland production was observed in some countries because of climatic variability and anomalies. In this study, we have shown that ORCHIDEE-GM is able of capturing the interannual variability of grassland productivity.

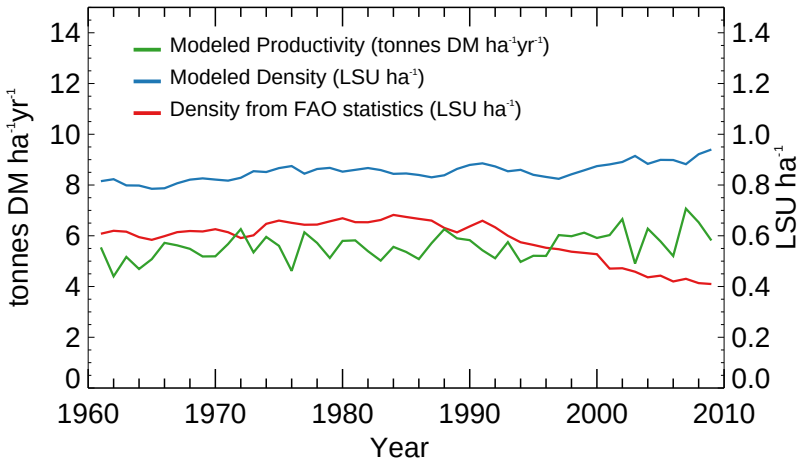

Figure 5. Temporal evolution of modelled grassland productivity, and of livestock density from model simulations and statistics respectively. All variables are means over European grasslands.

5. Grassland modelling in Brazil: first experiences with PaSim and ORCHIDEE-GM

This chapter documents the first modelling applications on Brazilian grasslands with PaSim and ORCHIDEE-GM. The modelling work was mainly developed in the course of the post-doctoral stage of Priscila Coltri, carried out at Laboratoire des Sciences du Climat et l'Environnement from 01/11/2012 to 11/07/2013.

PaSim

For PaSim, which has no specific equations for tropical plants, a first verification of model responses against tropical conditions was done to identify major weaknesses as a preparation for future calibration. The simulations run aimed at testing the model responsiveness under tropical conditions, under which this model had never been evaluated before. To achieve this, soil and plant data from *Brachiaria* (cv Marandu) swards were used as described in Lara (2011), for the site of Piracicaba (22° 25′ S, 47° 23′). Temperature, precipitation, solar radiation, wind speed and humidity inputs were supplied by ESALQ (Escola Superior de Agricultura "Luiz de Queiroz") - USP (Universidade de São Paulo) weather station (through http://www.esalq.usp.br) for the years 2007, 2008 and 2009.

Overall, simulations indicated that the model, while not adapted for simulating tropical conditions, responds appropriately to tropical conditions characterized by higher temperature and rainfall values than those found on temperate sites, without computational problems. Figures 1 shows the simulation results for four output variables: leaf area index (m^2 m^{-2}, graph a), dry matter (kg ha^{-1}, graph b), cumulative and daily evapotranspiration (mm, graphs c and d, respectively). The complete list of output variables is in appendix II.

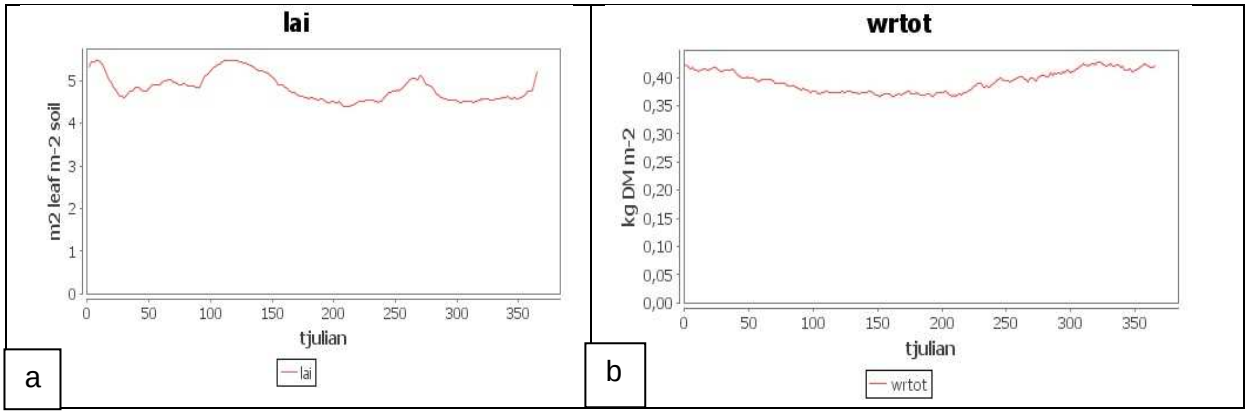

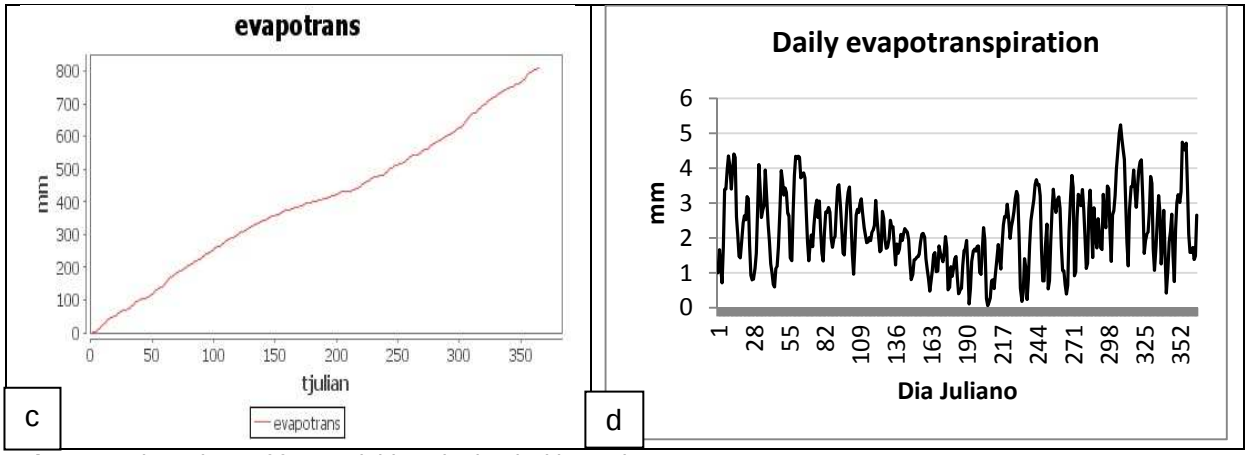

Figure 1. The values of four variables obtained with PaSim.

These results suggest, however, the need for improved plant physiology parameterization, especially with respect to carbon assimilation (photosynthesis and respiration) by the canopy. Moreover, the following equations were identified (as included in the model PlantMod, described by Johnson, (2012) for inclusion in the code of PaSim to extend its capabilities towards C4 species:

Equation of the response to carbon (CO_2), *fc(C)*:

$$f_c(C) = \frac{1}{2\emptyset}\left[\beta C + f_{c,m} - \{(\beta C + f_{c,m})^2 - 4\emptyset\beta f_{c,m} C\}^{\frac{1}{2}}\right] \quad (3)$$

where: C is the atmospheric concentration of carbon, β is an initial slope, ∅ (0≤ ∅ ≤ 1) is a curvature parameter, and f_(c,m) is an asymptotic function.

Equation of photosynthesis at light saturation, *Pm*:

$$P_{m=} P_{m,ref}\, fc\,(C) f_{pm,TC}(T,C)\, f_{pm,fp}\,(fp) \quad (4)$$

where $f_c(C)$ is the response function to CO_2, $f_{pm,TC}(T,C)$ is the temperature-CO_2 combined response, $f_{pm,fp}$ is the response to plant enzyme or protein concentration ($_{fp}$) mol of protein *C* (mo. leaf C)$^{-1}$ and $P_{m,ref}$ is the reference value for P_m concerning the temperature, CO_2 concentration in the atmosphere.

Equation of the temperature-CO_2 combined response:

$$f_{pm,TC}\,(T,C) = \left(\frac{T - T_{mn}}{T_{ref} - T_{mn}}\right)^q \left(\frac{(1+q)\,T_{opt} - T_{mn} - qT}{(1+q)\,T_{opt} - T_{mn} - qT_{ref}}\right) \quad (5)$$

Where T_{mn} is the minimum temperature, q is a curvature parameter, T_{ref} is the reference temperature, T_{opt} is the optimum temperature (related to carbon) and described according to equation:

$$T_{opt,Pm} = T_{opt,Pm,amb} + \gamma_{pm}[f_c\,(C) - 1] \quad (6)$$

where f_c is the functional of CO_2.

Equation on leaf photosynthetic efficiency: The general characteristics of photosynthetic efficiency in relation to temperature and CO_2 are:

- Efficiency increases with the increase in CO_2 concentration, although this increase is relatively modest in C4 plants;

- α decreases as the temperature rises above 15 °C (critical temperature above which α starts to decrease, with increasing CO_2 concentration) due to a shift from carboxylation (carbon fixation) to oxygenation (photorespiration) in the reactions of photosynthesis;

- The impact of temperature increase is reduced by the increase in CO_2 concentration;

- *α* increases in response to the concentration of protein;

In order to capture these responses, photosynthetic efficiency is given by:

$$C4: \alpha = \alpha_{amb,15} fc(C) f_{\alpha,fp}(fp) \quad (7)$$

where $\alpha_{amb,15}$ mol CO_2, *α* is the value of the atmospheric CO_2 concentration at 15 °C and the protein concentration reference with the default value.

These equations for C4 photosynthesis were identified and implemented in the PaSim code by INRA Grassland Ecosystem Research Unit of Clermont-Ferrand (France). Evaluations against EMBRAPA datasets are ongoing.

ORCHIDEE-GM

The model ORCHIDEE-GM implements equations for tropical C4 forage species, allowed the comparison of the simulated results with actual results. Climatic data from NCEP re-analyses were used to input the model.

To assess the responses of ORCHIDEE-GM, four variables were selected: leaf area index (LAI, m^2 m^{-2}), dry material production (kg ha^{-1}), leaf dry biomass (kg ha^{-1}) and specific leaf area (SLA, m^2 kg^{-1}). The following action strategy was followed:

1) First, the model was stabilized against tropical data. Soil and land use and occupancy inputs were extracted from the global soil sub-model of LPJ Dynamic Global Vegetation Model (http://www.pik-potsdam.de/research/projects/lpjweb) and positioned to the latitude and longitude of the study area, choosing to PFT (Plant Functional Type) option for tropical C4 plant species.

The results from this first simulation (Figure 2), carried out with GM-ORCHIDEE (based on data from Araujo, 2011), show that herbage mass (dry matter) values are slightly higher and the values of leaf area index slightly lower than expected. As well as PaSim, the model reproduces seasonal climate variability of São Carlos (in São Paulo State). Figure 2 shows that herbage mass (dry matter), as well as leaf area index (LAI) and net primary production (NPP) are lower in the driest time of year, which runs from June to September. Moreover, these variables begin to increase in October, at the onset of the rainy season, remaining high until the next dry season.

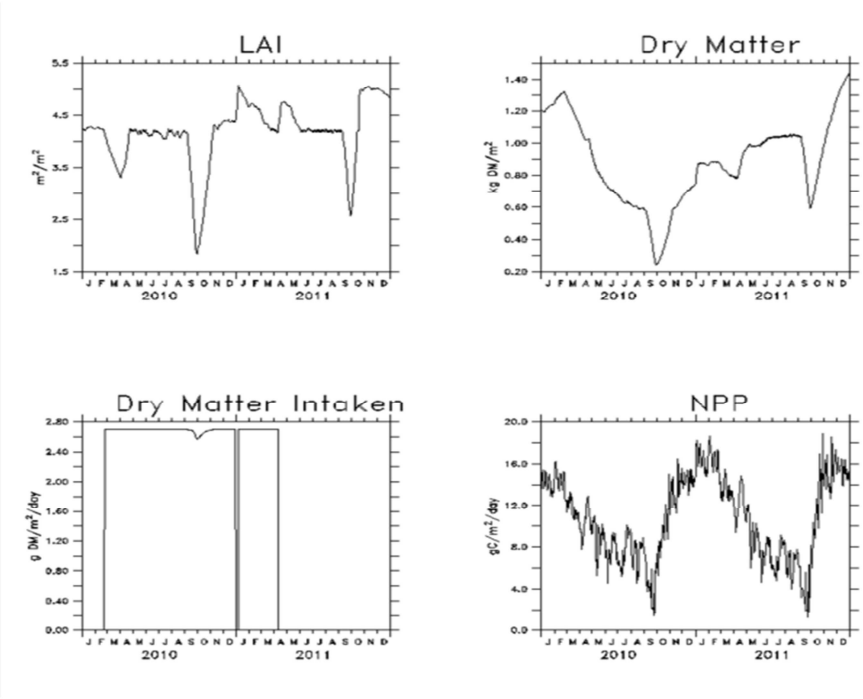

Figure 2. Results of the first round of ORCHIDEE-GM simulations for the city of São Carlos, São Paulo: a, Leaf Area Index (LAI); b, dry matter; c, dry matter intake for cattle, and d, net primary productivity (NPP).

2) Second, management data and forage characteristics of the study area, located in the municipality of São Carlos, were introduced as described in Araujo (2011). In this simulation, the forage grass *Panicum maximum* cv. Mombaçan was chosen, with maximum leaf area index (LAI) of 8.27 and plant height of 0.90 m. The management of the forage sward is shown in Table 2, in Julian days, as needed by the ORCHIDEE-GM. In this simulation, we also parameterized the shadow effect, used in the model. In temperate locations, the forage plant starts responding to self-shading when LAI=2.5. However, the same does not occur in tropical locations, where this parameter was set to 4.2.

To perform the simulation, we chose four PFTs:

a) PFT1: exposed soil;

b) PFT2: natural forest in the region;

c) PFT3: cutting management of pasture (simulation results were compared against actual data from Araújo (2011);

d) PFT4: management with grazing cattle, with 2.08 animal units per ha per year, which is the average of the west of São Paulo State, according to the IBGE - Instituto Brasileiro de Geografia e Estatística (http://www.ibge.gov.br).

It was found a need to improve parameter estimates, particularly with regard to production. Moreover, it was observed that the Soil Tillage Intensity Rate (stir), taken from a global database do not represent the water retention and the characteristics of the study area.

Simulation data were compared against actual field data (Araujo, 2011). Figure 3 shows the simulation for the leaf area index (LAI). In this figure it can be seen that the model reproduces the LAI quite reliably, with correlation and concordance index of 0.76 (p<0.001).

The reproduction of the actual LAI was better in summer, fall and spring seasons, which are not dry months. In these months, the correlation was higher than 0.8 (p<0.001), and the simulation was better in summer, with correlation of 0.9. Thus, it was concluded that ORCHIDEE-GM best simulates the summer, autumn and spring phases of LAI. In winter, that is the dry season in that region, the model tends to overestimate LAI values.. Table 4 shows the values of the statistical analyses of the simulated data versus actual data. It is possible to note that the lowest correlation (0.44) between actual and simulated data occurred during the dry season in winter.

Importantly, ORCHIDEE-GM also simulates adequately the magnitude of values, including plant regrowth after cutting. In Figure 3 the plant growing cycles with the trajectories of LAI are presented, in which discontinuities are related to the cut events.

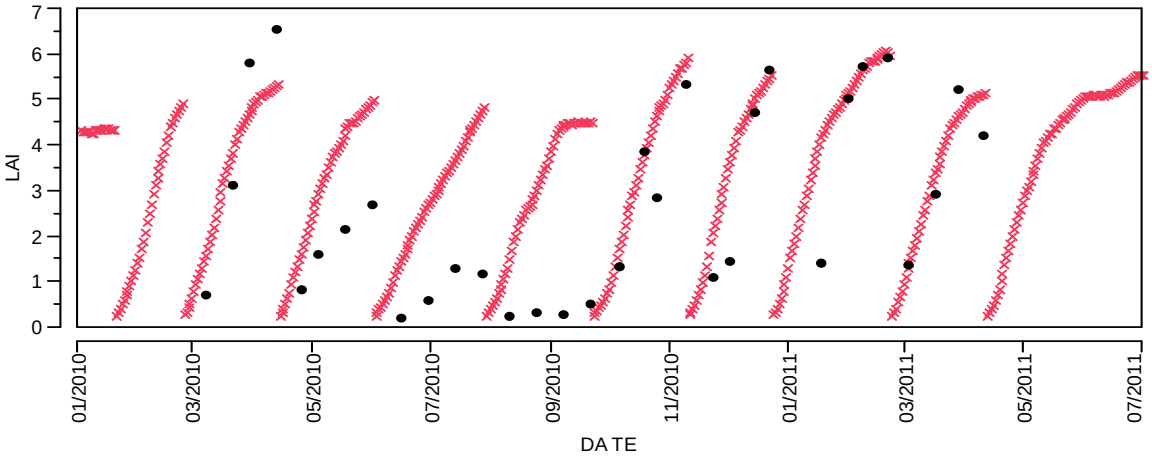

Figure 3. Leaf area index (LAI) simulated by ORCHIDEE-GM (in red) compared to actual data (in black).

Table 4. Statistical indices of LAI simulated by ORCHIDEE-GM and actual LAI data (Araujo, 2011).

Data	Correlation	RMSE (m^2 m^2)	Index of agreement (IOA)	Observation (n)
2010-2011	0.76	1.79	0.76	32
Summer	0.90	1.07	0.97	8
Autumn	0.83	1.38	0.83	10
Winter	0.44	3.04	0.20	7
Spring	0.87	1.23	0.84	7

Figure 4 shows the amounts of biomass of leaves (kg ha^{-1}) simulated by ORCHIDEE-GM and compared with the actual leaf biomass were collected in the field. As the LAI, the model was able to reproduce faithfully the actual data, with overall correlation of 0.77 and concordance index of 0.79 (Table 5). Also like the LAI, the lowest correlation occurred in winter (0.73). However, the correlation between simulated and actual values of biomass was better than LAI. The best correlation, together with the lowest estimation error (RMSE), occurred in spring (correlation = 0.9, p<0.001). The concordance index shows that, both in spring and autumn, the simulated results are close to the actual data, with IOA=0.87.

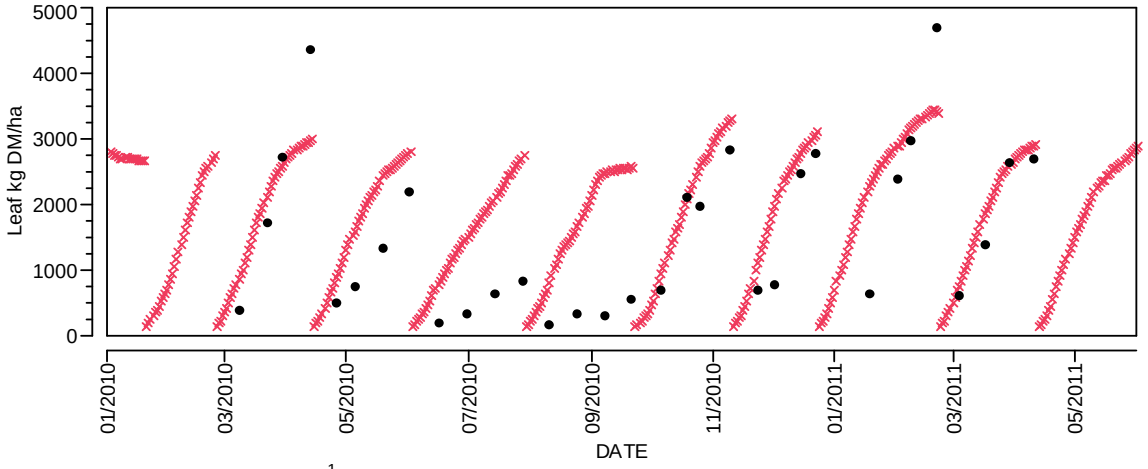

Figure 4. Leaf biomass (kg ha^{-1}) simulated by ORCHIDEE-GM (in red) compared to the actual data (in black).

Table 5 - Statistical indices calculated with leaf biomass simulated by ORCHIDEE-GM and actual leaf biomass.

Data	Correlation	RMSE (kg leaf DM ha^{-1})	Index of agreement (IOA)	Observations (n)
2010-2011	0.77	987.08	0.79	32
Summer	0.85	829.72	0.94	8
Autumn	0.87	714.02	0.87	10
Winter	0.73	1599.09	0.23	7
Spring	0.90	617.9	0.87	7

Figure 5 presents data of dry matter (kg ha^{-1}) simulated by ORCHIDEE-GM and compared with actual observations. Although statistical analyses show high correlations, at all times of the year, there is overestimation of pattern. The model can reproduce regrowth and a large amount of dry matter in the rainy season as it happens with actual data, which explains the high correlation. However, the simulated values are higher than observed values. The RMSE, which is the error of the model, exceeds 3.000 kg ha^{-1} at all stages of the year, reaching a value of 11082.3 kg ha^{-1} in winter. As for LAI and leaf biomass, the model gives worse results in winter.

The fact that the model error is high, explains the low concordance rates that were less than 0.6 in all seasons. Table 6 presents the statistical analyses performed.

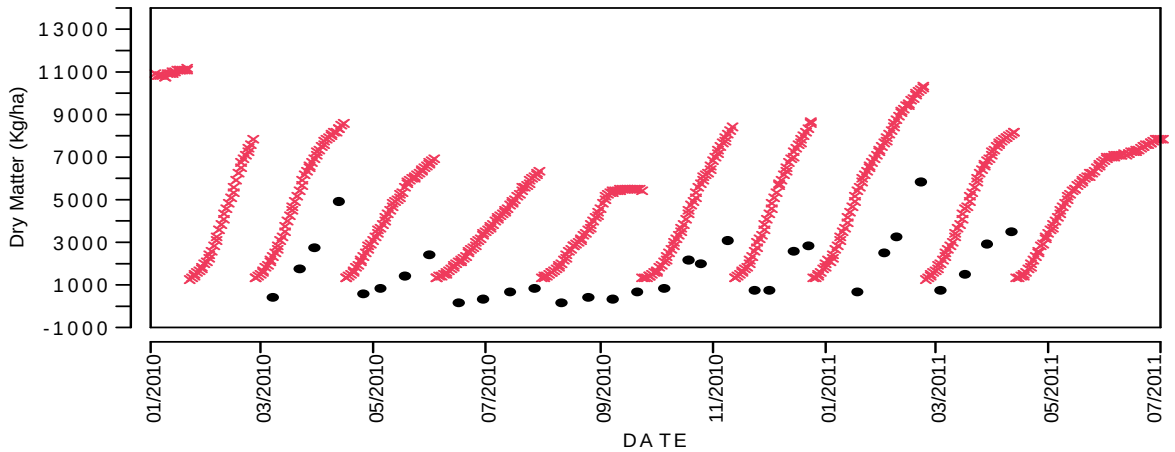

Figure 5. Dry matter (kg ha^{-1}) simulated by ORCHIDEE-GM (in red) compared to the actual data (in black).

Table 6. Statistical indices calculated with simulated dry biomass by ORCHIDEE-GM and actual dry biomass.

Data	Correlation	RMSE (kg ha^{-1})	Index of agreement (IOA)	Observations (n)
2010-2011	0.86	3910.4	0.5	32
Summer	0.88	4921.35	0.38	8
Autumn	0.93	3672.6	0.5	10
Winter	0.79	11082.3	0.1	7
Spring	0.89	3612.47	0.40	7

Figure 6 shows the data of specific leaf area (SLA), in g cm^{-2}, simulated by ORCHIDEE-GM and actual data. In this case, the model does not simulate the variations of specific surface area at any stage of the year. ORCHIDEE-GM model cannot simulate such a broad variation in SLA. Statistical analyses indicate low correlations and high errors, in as Table 7.

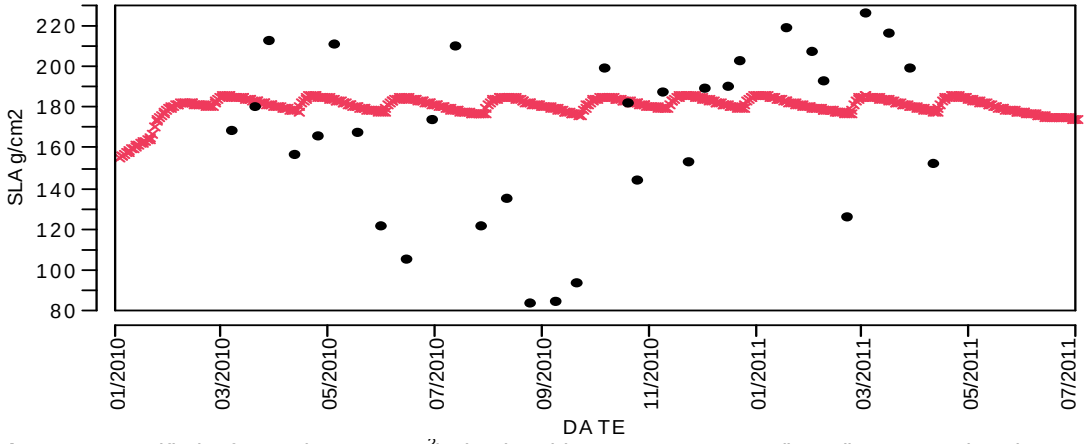

Figure 6. Specific leaf area (SLA, g cm^{-2}) simulated by ORCHIDEE-GM (in red) compared to the actual data (in black).

Table 7 - Statistical indices calculated with dry biomass simulated by ORCHIDEE-GM and actual dry biomass.

Data	Correlation	RMSE (kg ha^{-1})	Index of agreement (IOA)	Observations (n)
2010-2011	0.28	41.83	0.32	32
Summer	0.51	33.01	0.98	8
Autumn	0.13	35.9	0.36	10
Winter	0.06	67.12	0.45	7
Spring	-0.11	20.15	0.23	7

3) Third, simulations were run with modified values of soil parameters, after the data analysis and soil description from Araujo (2011) while the other inputs were kept as in the analysis reported above. We referred to a Yellow dystrophic Oxisol soil, which is usually more than two meters deep, with 72.5% of sand, 23.5% of clay and 4.0% of silt. Other soil data were used as described in Table 3. As in the second simulation, Specific Leaf Area (SLA) values obtained with ORCHIDEE-GM were weakly correlated with the actual data, in this simulation SLA parameter values were also changed (maximum SLA=226.67g cm^{-1}, minimum SLA=83.25 g cm^{-1}).

Statistical analyses of the second and third simulations were first performed for the entire dataset, and then separated into summer (from 21/12 to 21/03), autumn (22/03 to 20/06), winter (21/06 to 21/09) and spring (22/09 to 20/12).

Table 2. Cycles of sprouting and cutting days (based on data described in Araujo, 2011).

Growth cycles	Beginning	End – Cutting day	Days of cycle
1	23 Feb. 2010 (JD: 54)	13 Apr. 2010 (JD: 103)	49
2	13 Apr. 2010 (JD: 103)	01 Jun. 2010 (JD: 152)	49
3	02 Jun. 2010 (JD: 153)	28 Jul. 2010 (JD: 209)	56
4	28 Jul. 2010 (JD: 209)	21 Sep. 2010 (JD: 264)	55
5	22 Sep. 2010 (JD: 265)	9 Nov. 2010 (JD: 313)	48
6	10 Nov. 2010 (JD: 314)	22 Dec. 2010 (JD: 356)	42
7	07 Jan. 2011 (JD: 7)	21 Feb. 2011 (JD: 52)	45
8	22 Fev. 2011 (JD: 53)	11 Abr. 2011 (JD: 101)	48

*JD = Julian Day

Table 3. Physical properties of the soil used in the second simulation (based on data described in Araujo 2011).

Property	Depth (cm)					
	0-10	10-20	20-30	30-40	40-50	50-60
Total density of clay (g cm^{-3})	1.30	1.39	1.44	1.48	1.54	1.56
Upper limit of saturation at 0.0 Mpa (g kg^{-1})	500	470	450	440	410	410
Field capacity at 0.0 Mpa (g kg^{-1}) at 0.01 Mpa (g kg^{-1})	265	227	223	235	252	255
Permanent wilting point at 1.5 Mpa (g kg^{-1})	156	133	137	154	164	171

Figure 7 shows the comparison of actual LAI with the third simulation. In this case, an improvement was observed during the winter season only (Figure 8), and the correlation increased considerably, from 0.44 to 0.79, which also resulted in a higher overall correlation, rising to 0.79. Although the improvement was important, LAI data are still overestimated in winter. There was also a small improvement in the months of March and April, which is the result of the amount of water that the "new soil" model, represented by actual data, retained water. It is worth stressing that although both overall and winter correlations have increased, the RMSE also increased from 1.7 to 1.9.

Table 9 shows the seasonal statistical analysis of the data.

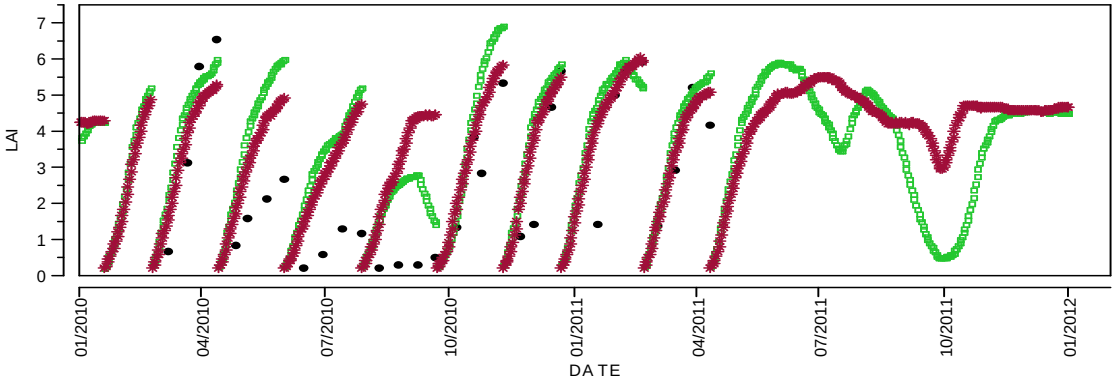

Figure 7. Data from simulated leaf area index with the observed soil data (in green), simulated with the file global soil (in red) and real data (black).

Table 8. Statistical indices calculated simulated LAI by ORCHIDEE-GM and actual data.

Variables	Correlation and p-value	Correlation of Spearman and p-value	Index of agreement (IOA)	RMSE	N
LAI x 2ª simulation	0.7571 (p>0.0001)*	0.7687 (p>0.0001)*	0.7647	1.796	32
LAI x LAI –3a simulation	0.7924 (p>0.0001)*	0.7988 (p>0.0001)*	0.7671	1.931	32

* Significant at 0.05.

Table 9. Seasonal statistical indices calculated with simulated LAI by ORCHIDEE-GM and actual data..

Data	Correlation		RMSE m^2/m^2		Index of agreement (IOA)		N
LAI	2a simulation	3a simulation	2a simulation	3a simulation	2a simulation	3a simulation	
Summer	0.90	0.83	1.07	1.40	0.97	0.94	8
Autumn	0.83	0.76	1.38	1.91	0.83	0.74	10
Winter	0.44	0.79	3.04	2.52	0.20	0.30	7
Spring	0.87	0.83	1.23	1.78	0.84	0.77	7

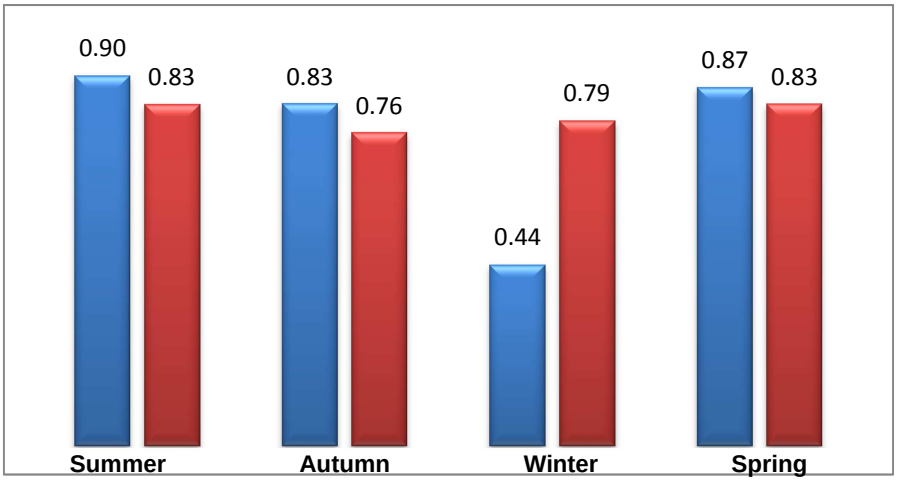

Figure 8. Comparison between the correlations of the simulations with ORCHIDEE-GM in four seasons. Blue and red bars correspond to the second and third simulations, respectively.

Figure 9 shows the third simulation of dry matter (kg ha^{-1}) performed with soil data of the study area compared to the second simulation, obtained with actual data. The overall correlation (Table 10) shows a higher correlation of the new simulation data, compared to the results of previous simulation. Although the seasonal correlations have not shown any improvement (Table 11), the average relative error (RMSE) decreased in winter (Figure 10), which made the overall correlation increased. Although this simulation error of winter was lower, yet the model still overestimates the total dry matter (Figure 9), especially in winter.

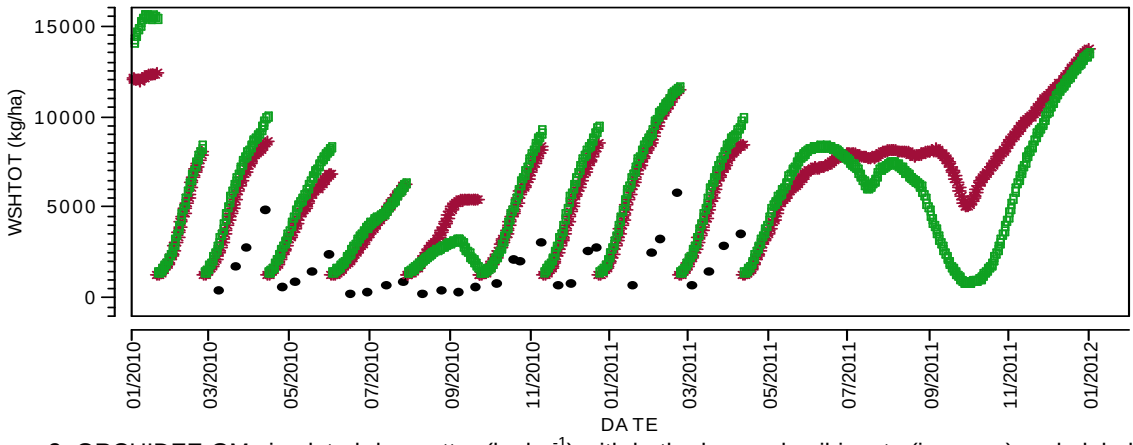

Figure 9. ORCHIDEE-GM simulated dry matter (kg ha^{-1}) with both observed soil inputs (in green) and global soil inputs (in red), and actual data (black).

Table 10. Statistical indices calculated with simulated dry matter by ORCHIDEE-GM and actual data.

Variables	Correlation and p-value	Correlation of Spearman and p-value	Index of agreement (IOA)	RMSE (kg ha^{-1})	n
Actual DM x 2a simulation	0.8713 (p>0.0001)	0.8541 (p>0.0001)	0.49	4121.7	32
Actual DM x 3a simulation	0.8920 (p>0.0001)	0.8852 (p>0.0001)	0.47	4443.5	32

Table 11 – Seasonal indices calculated with simulated dry matter by ORCHIDEE-GM and actual data.

Dry matter data	Correlation		RMSE (m^2 m^{-2})		index of agreement indicator (IOA)		N
	2a simulation	3a simulation	2a simulation	3a simulation	2a simulation	3a simulation	
Summer	0.89	0.87	4886.3	5279.06	0.34	0.29	8
Autumn	0.93	0.93	3805.14	4636.7	0.49	0.43	10
Winter	0.79	0.66	4075.77	3192.8	0.10	0.13	7
Spring	0.9	0.85	3616.37	4183.8	0.40	0.36	7

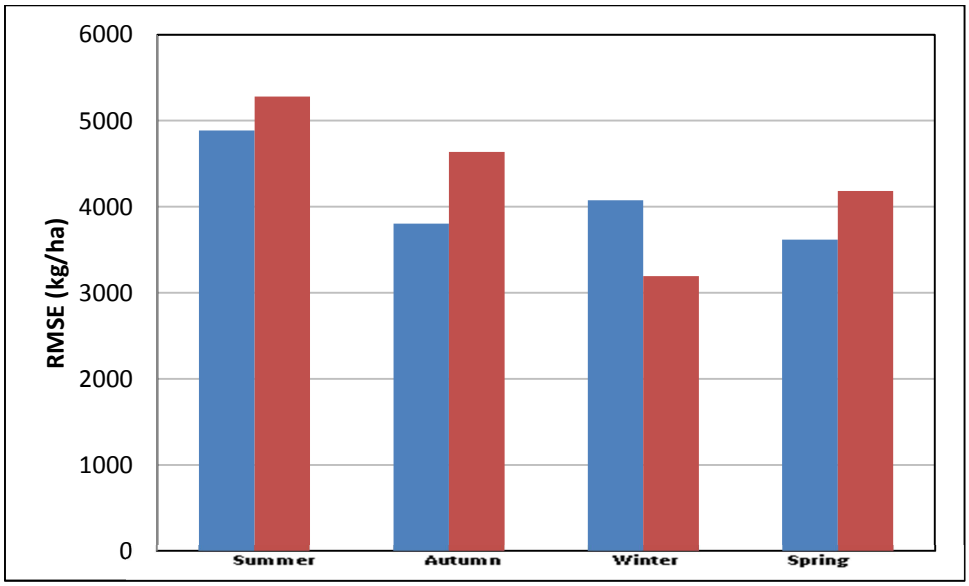

Figure 10. Comparison of mean relative error (RMSE) obtained with ORCHIDEE-GM simulations in four seasons. Blue and red bars correspond to the second and third simulations, respectively.

Figure 11 shows the third simulation of dry matter (kg ha^{-1}) performed with soil data of the study area compared to the second simulation. As occurred with the total dry matter, the model showed better results in winter and there was an increased correlation in the season. This improvement was also observed in the overall correlation (Table 12). Table 13 presents the seasonal statistical analyses. Figure 12 shows the seasonal correlations.

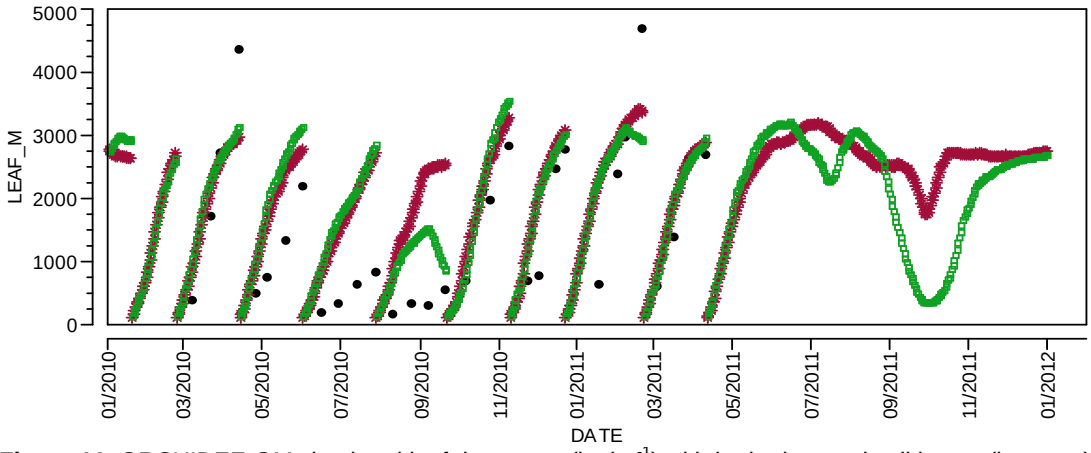

Figure 11. ORCHIDEE-GM simulated leaf dry matter (kg ha^{-1}) with both observed soil inputs (in green) and global soil inputs (in red), and actual data (black).

Table 12. Statistical indices calculated with simulated leaf dry matter by ORCHIDEE-GM and actual data.

Variables	Correlation and p-value	Correlation of Spearman e and p-value	Index of agreement (IOA)	RMSE (kg ha^{-1})	n
Leaf dry matter x 2a simulation	0.7758 (p>0.0001)*	0.8438 (p>0.0001)*	0.79	987.08	32
Leaf dry matter x 3a simulation	0.7918 (p>0.0001)*	0.8621 (p>0.0001)*	0.80	929.7	32

Table 13. Seasonal statistical indices calculated with simulated leaf dry matter by ORCHIDEE-GM and actual data.

Leaf dry matter data	Correlation		RMSE (kg DM ha^{-1})		Index of agreement (IOA)		n
	2a simulation	3a simulation	2a simulation	3a simulation	2a simulation	3a simulation	
Summer	0.85	0.78	829.72	942.8	0.94	0.93	8
Autumn	0.87	0.83	714.02	817.10	0.87	0.83	10
Winter	0.73	0.76	1599.09	1236.4	0.23	0.32	7
Spring	0.90	0.89	617.9	673.3	0.87	0.86	7

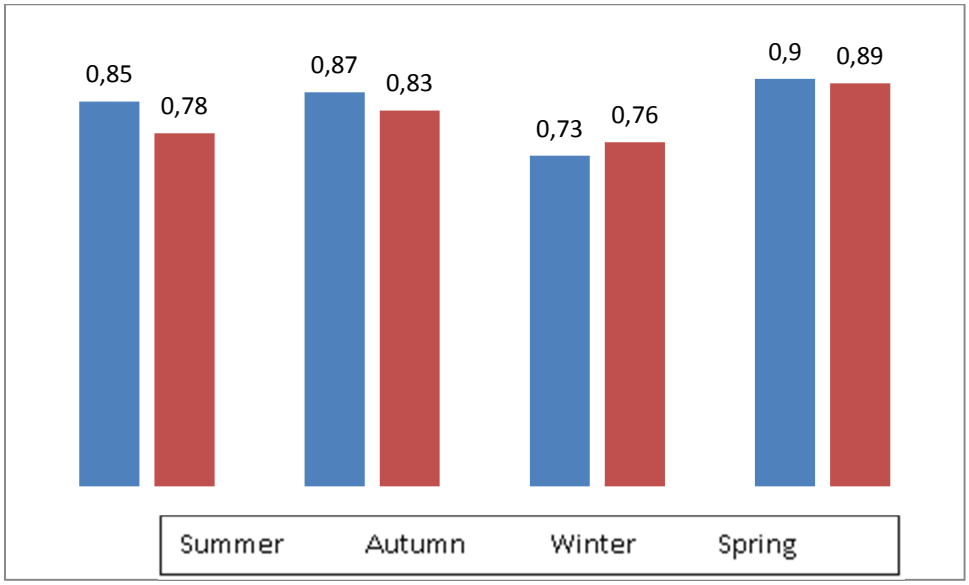

Figure 12. Comparison between the correlations of the simulations with ORCHIDEE-GM in four seasons. Blue and red bars correspond to the second and third simulations, respectively.

Figure 13 shows simulation results of specific leaf area (2nd and 3rd simulations) compared to the simulation results obtained with actual data. Although this third simulation has shown better results, the simulation is still far from the actual data. Between the 2nd and 3rd simulation, that there was progress and the third simulation data are more compatible with actual data variations. Also, in winter, the simulation shows a decrease as well as in the actual data. However, simulation data still fail to reproduce the high variation that actual specific leaf area shows.

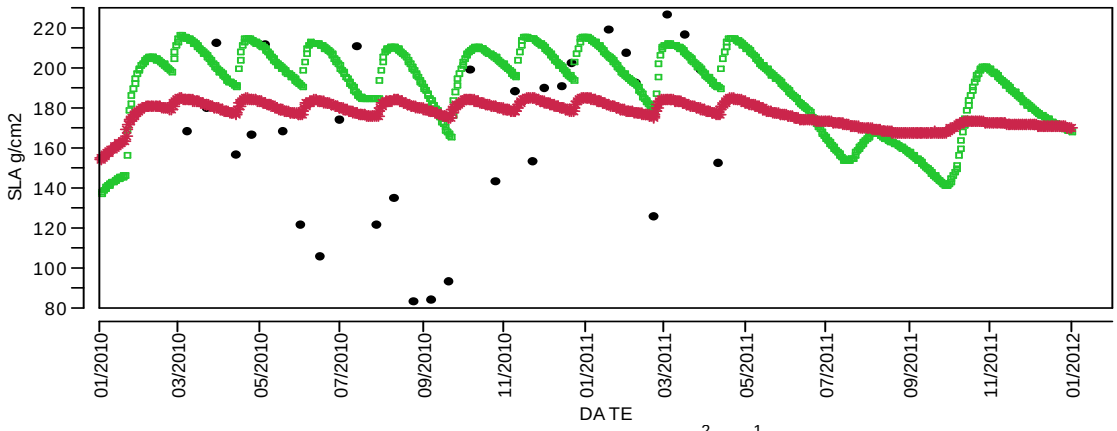

Figure 13. ORCHIDEE-GM simulated specific leaf areas (SLA, m^2 kg^{-1}) with both observed soil inputs (3rd simulation, in green) and global soil inputs (2nd simulation, in red), and actual data (black).

Table 14. Statistical indices calculated with simulated specific leaf area by ORCHIDEE-GM and actual data.

Variables	Correlation and p-value	Correlation of Spearman and p-value	Index of agreement (IOA)	RMSE ($g\ cm^{-2}$)	n
SLA x before results	0.2838 (p>0.1154)	0.2721 (p>0.1320)	0.32	41.83	32
SLA -from the observation data	0.4099 (p>0.0198)	0.2782 (p>0.1231)	0.49	48.54	32

Table 15. Seasonal statistical indices calculated with simulated specific leaf area by ORCHIDEE-GM and actual data.

SLA data	Correlation		RMSE (g cm^{-2})		Index of agreement (IOA)		n
	2a simulation	3a simulation	2a simulation	3a simulation	2a simulation	3a simulation	
Summer	0.51	0.59	33.01	26.35	0.98	0.99	8
Autumn	0.13	0.13	35.9	47.43	0.36	0.45	10
Winter	0.06	0.26	67.12	74.4	0.45	0.46	7
Spring	-0.11	-0.32	20.15	35.02	0.23	0.41	7

Conclusions

Advancements in tropical grassland modelling with two models - PaSim and ORCHIDEE-GM - have been presented. For PaSim, this activity opened to the introduction in its code of equations governing the photosynthesis of C4 plants. ORCHIDEE-GM was tested in Brazil for the first time, which consisted in a complete diagnostic analysis. The model showed good performances against actual data. The best results were obtained with leaf outputs (leaf area index and leaf dry matter). The simulation of total dry matter showed an overestimation of this variable, especially in winter. The results also showed that the model cannot simulate sudden variations in specific leaf area.

The partnership between Brazilian and French institutions has favoured the generation of a flow of ideas, allowing for advancements with the use of PaSim and ORCHIDEE-GM for areas of Brazilian beef production, complying with AnimalChange objectives.

6. Calibration and validation of crop models SWB-SCI and STICS in South Africa

The crop models SWB-SCI (Annandale *et al.*, 1999) and STICS (Brisson *et al.*, 2003) were calibrated and validated for maize (*Zea mays* L.) (PAN6977) and weeping lovegrass (*Eragrostis curvula* (Schrad.) Nees) using data collected from controlled experimental plots. The experimental plots are located at the East Rand Water Care Works (ERWAT), Johannesburg, Gauteng, South Africa. The study site is situated at an elevation of 1577 m above sea level, latitude 26° 01' 01" S and longitude of 28° 16' 55" E. The total annual rainfall of the area ranged between 405 mm in 2006-2007 and 710 mm in 2007-2008, mainly during the months of October to March. The soil of the experimental site is a clay loam, Hutton soil form (Soil Classification Working Group, 1991) having an average clay content of 38%, and pH (H_2O) of 5.73.

The accuracy of model simulations was assessed based on a set of performance measures (Table 1), using the reliability criteria proposed by De Jager (1994).

Table 1. Model performance measures and criteria for reliability (after De Jager, 1994).

Performance measure	Unit	Value range and purpose	Reliability criteria
Coefficient of determination (r^2) of the linear regression estimates versus measurements	dimensionless	0 (absence of fit) to 1 (perfect fit): the closer values are to 1, the better the model	> 0.8
Willmott (1982) index of agreement (d)	dimensionless	0 (absence of agreement) to 1 (perfect agreement): the closer values are to 1, the better the model	> 0.8
Root mean square error (RMSE)	unit of the variable	0 (optimum) to positive infinity: the smaller RMSE, the better the model performance	-
Mean absolute error over the mean of the measured values (MAE(%))	%	0 (optimum) to positive infinity: the smaller MAE(%), the better the model performance	< 20

SWB-SCI crop model

Model calibration

Model parameters such as specific leaf area, leaf stem partitioning factor, thermal time requirements, maximum root depth, maximum crop height, dry matter water ratio, radiation

use efficiency, extinction coefficient, stem to grain translocation, top dry matter at emergence, harvestable dry matter, and maximum grain N concentration for maize (*Zea mays* L.) (Table 1) and a planted perennial pasture, the weeping lovegrass (*Eragrostis curvula* (Schrad.) Nees) (Table 2), were determined from field data. All remaining parameters were set according to literature values.

Table 1. Model parameters for medium season maize cultivar (PAN6966).

Parameter	Unit	Value	Source
Canopy radiation extinction coefficient	dimensionless	0.57	Field measurement
Vapour pressure deficit corrected dry matter water ratio	Pa	9.4	Field measurement
Radiation conversion efficiency	Kg MJ^{-1}	0.00220	Field measurement
Specific leaf area (SLA)	m^2 kg^{-1}	15	Field measurement
Base temperature	(^oC)	10	Bunting (1976)
Temperature for optimum growth	(^oC)	25	Keeling and Greaves (1990), Shaw (1983), McMaster and Wilhelm, (1997), Kenny and Harrison (1992)
Cut off Temp.	(^oC)	30	Hensley *et al.* (1994)
Thermal time requirement for emergence	degree days	50	Field measurement
Thermal time at end of vegetative stage	degree days	1000	Field measurement
Thermal time requirement for maturity	degree days	1700	Field measurement
Thermal time for transition period	degree days	10	Field measurement
Leaf senescence	degree days	1300	Field measurement
Maximum crop height	m	3.20	Field measurement
Maximum root depth	m	1.60	Field measurement
Fraction of total dry matter translocated to heads	dimensionless	0.05	Hensley *et al.* (1994)
Leaf water potential at maximum transpiration	kPa	-2000	Hensley *et al.* (1994)
Maximum transpiration	mm d^{-1}	9	Hensley *et al.* (1994)
Leaf stem partitioning	m^2 kg^{-1}	0.8	Hensley *et al.* (1994)
Total dry matter at emergence	kg m^{-2}	0.0019	Field measurement
Fraction of total dry matter partitioned to roots	dimensionless	0.2	Hensley *et al.* (1994)
Root growth rate	m2 kg^{-1}	8	Hensley *et al.* (1994)
Stress index	dimensionless	0.95	Hensley *et al.* (1994)

Table 2. Crop parameters for weeping lovegrass (*Eragrostis curvula* (Schrad.) Nees).

Parameter	Unit	Value	Source
Canopy radiation extinction coefficient	dimensionless	0.90	Field measurement
Vapour pressure deficit corrected dry matter water ratio	Pa	4.0	Field measurement
Radiation conversion efficiency	Kg MJ^{-1}	0.00150	Field measurement
Specific leaf area (SLA)	m^2 kg^{-1}	8.00	Field measurement
Base temperature	(^oC)	10	Cox *et al.* (1988),

			Dalrymple (1976)
Temperature for optimum growth	(^{o}C)	20	Barnard *et al.*(1998)
Cut off Temp.	(^{o}C)	30	Barnard *et al.*(1998)
Thermal time requirement for emergence	degree days	0	Established
Thermal time at end of vegetative stage	degree days	700	Field measurement
Thermal time requirement for maturity	degree days	1500	Field measurement
Thermal time for transition period	degree days	10	Field measurement Barnard *et al.* (1998)
eaf senescence	degree days	700	Field measurement
Maximum crop height	m	0.3	Field measurement
Maximum root depth	m	1.4	Field measurement Barnard *et al.* (1998)
Fraction of total dry matter translocated to heads	dimensionless	0.01	Barnard *et al.* (1998)
Leaf water potential at maximum transpiration	kPa	-1500	Barnard *et al.* (1998)
Maximum transpiration	mm d^{-1}	9	Barnard *et al.* (1998)
Leaf stem partitioning	m^2 kg^{-1}	0.1	Field measurement
Total dry matter at emergence	kg m^{-2}	0.05	Field measurement
Fraction of total dry matter partitioned to roots	dimensionless	0.05	Barnard *et al.*(1998)
Root growth rate	m^2 kg^{-1}	4	Barnard *et al.* (1998)
Stress index	dimensionless	0.95	Barnard *et al.* (1998)

NB. The grass was cut just at flowering stage and the model was programmed to start initialise thermal time at zero after each cut because the crop is perennial.

A dataset containing field measurements of total aboveground biomass (t ha^{-1}) and leaf area index (m^2 m^{-2}) dynamics as well as grain yield (t ha^{-1}) were used to test the success of model calibration. The accuracy of model simulations was assessed based on a set of performance measures (Table 3), using the reliability criteria proposed by De Jager (1994).

Table 3. Model performance measures and criteria for reliability (after De Jager, 1994).

Performance measure	Unit	Value range and purpose	Reliability criteria
Coefficient of determination (r^2) of the linear regression estimates versus measurements	dimensionless	0 (absence of fit) to 1 (perfect fit): the closer values are to 1, the better the model	> 0.8
Willmott (1982) index of agreement (d)	dimensionless	0 (absence of agreement) to 1 (perfect agreement): the closer values are to 1, the better the model	> 0.8
Root mean square error (RMSE)	unit of the variable	0 (optimum) to positive infinity: the smaller RMSE, the better the model performance	-
Mean absolute error over the mean of the measured values (MAE(%))	%	0 (optimum) to positive infinity: the smaller MAE(%), the better the model performance	< 20

Generally, the model was calibrated successfully for both maize and weeping lovegrass (Figure 1), because the performance measures were all within the ranges prescribed by De Jager *et al.* (1994) (Table 4).

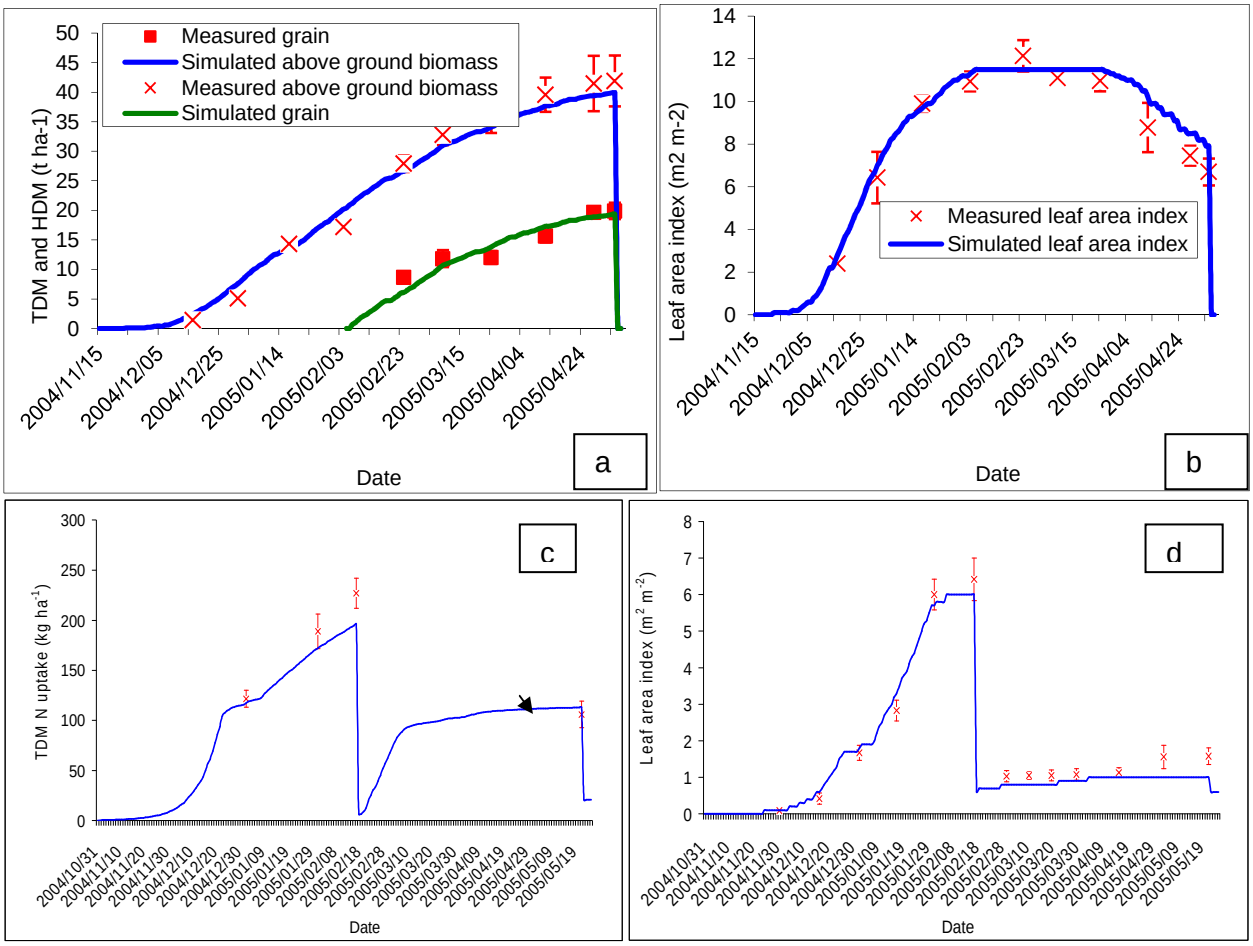

Figure 1. Simulated (solid lines) and measured values (symbols with standard deviation) for maize aboveground biomass (TDM) and grain yield (HDM) (a), maize leaf area index (b), weeping lovegrass hay yield (c), and weeping lovegrass leaf area index (d).

Table 4. Performance measures of the SWB-SCI model calibration simulations for maize and weeping lovegrass during the 2004/05 growing season.

Variable	n	d	RMSE	MAE (%)	r^2
Maize					
LAI	10	0.94	0.82	7.79	0.98
Aboveground biomass	10	0.98	2.18	7.40	0.99
Grain	6	0.88	1.72	9.72	0.95
Weeping lovegrass					
LAI	13	0.98	0.34	14.24	0.99
Aboveground biomass	13	0.92	0.89	15.81	0.97

Model corroboration

Model corroboration was conducted using variables from independent data sets collected during the 2004-2005 to 2007-2008 growing seasons for maize and weeping lovegrass. The

variables used to evaluate the accuracy of the model were LAI, aboveground biomass and grain (agronomic crops) yield.

Maize

Generally, the evaluation of the model against three-year combined independent data was more accurate for irrigated than dryland maize (Table 5). Under dryland maize cropping system, both aboveground biomass production and leaf area index were slightly overestimated for the first and last years (Figure 2). Grain yield was, however, estimated with acceptable accuracy. Nonetheless, the performance metrics for both aboveground biomass and grain yield were within acceptable accuracy ranges, with the exception of MAE for leaf area index, which was higher by 9% above the acceptable limit (Table 5). The model predicted irrigated maize aboveground biomass and grain yield with greater accuracy (Figs. 3; Table 5).

Table 5. Performance measures from simulations with SWB-SCI after calibration for maize and weeping lovegrass using combined data collected during the 2004-2005 to 2007-2008 growing seasons.

Variables	n	d	RMSE	MAE (%)	r^2
Dryland maize well fertilized treatment					
LAI	11	0.80	0.38	29	0.98
Aboveground biomass	16	0.87	2.37	20	0.99
Grain	10	0.87	1.10	20	0.91
Irrigated maize well fertilized treatment					
LAI	23	0.94	0.71	18	0.96
Aboveground biomass	29	0.94	2.69	15	0.97
Grain	18	0.92	1.59	16	0.97

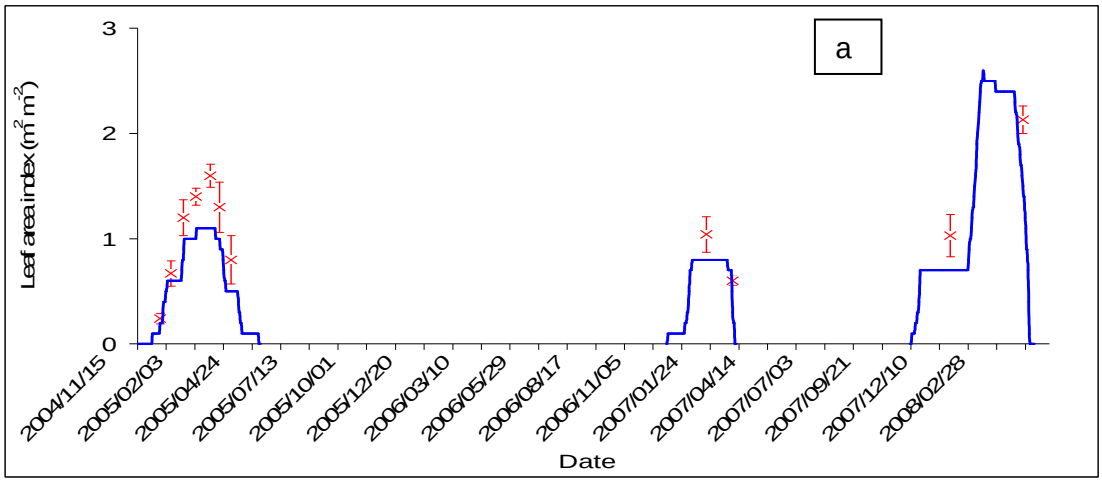

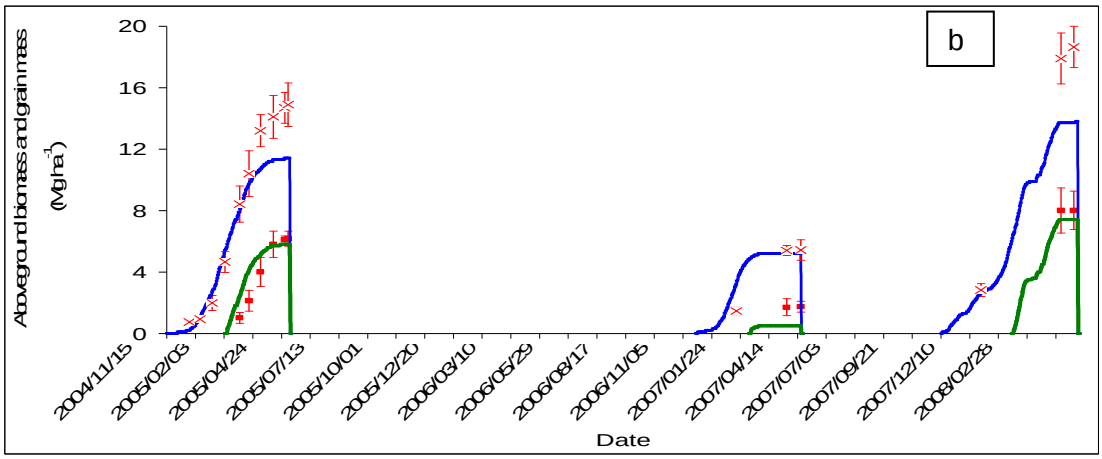

Figure 2. Simulated (solid lines) and measure values (symbols) of leaf area index (a) and aboveground biomass (blue line), grain yield (green line) (b) for maize planted under dryland with optimal fertilization during the 2004-2005 to 2007-2008 growing seasons.

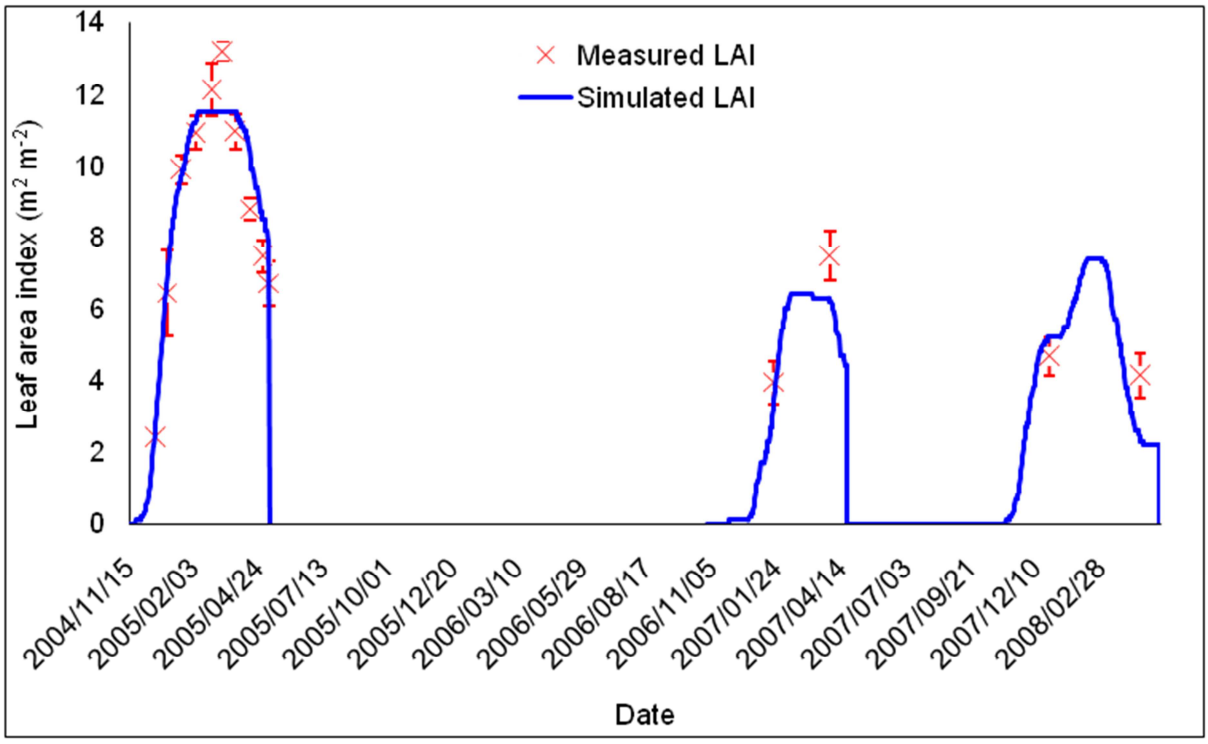

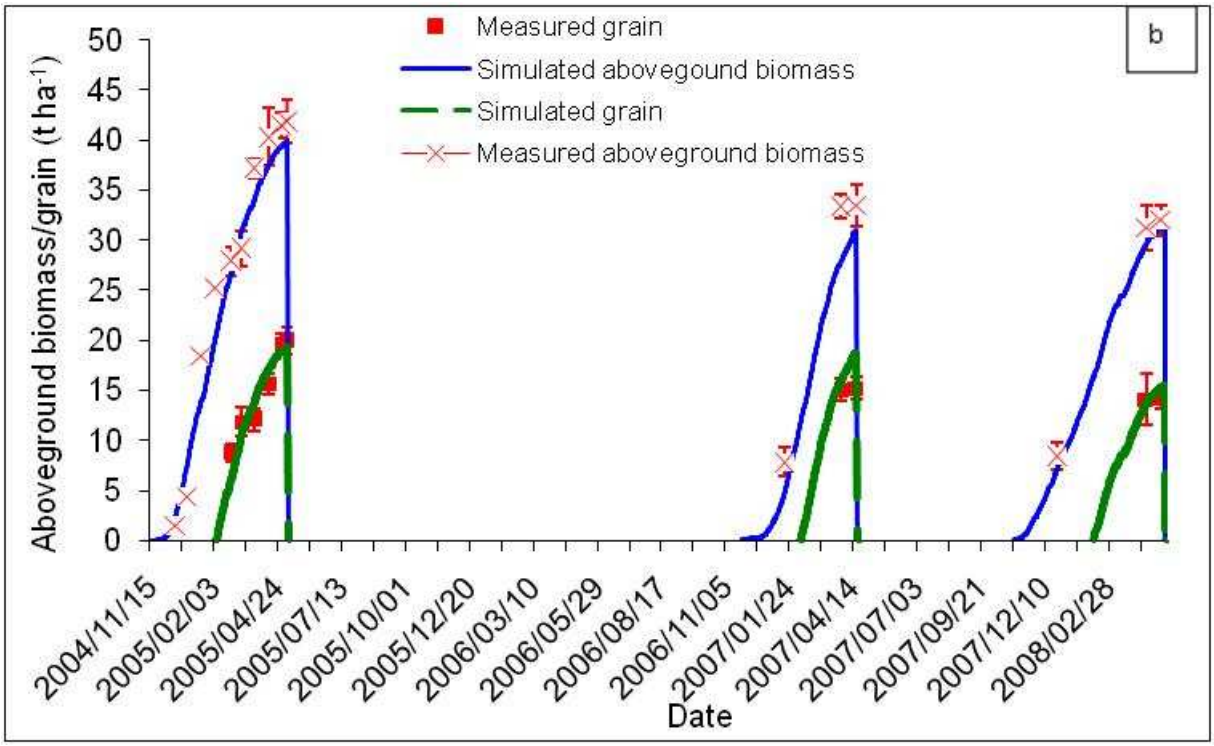

Figure 3. Simulated (solid lines) and measured values (symbols) of leaf area index (a) and aboveground biomass (blue line), grain yield (green line) (b) for irrigated maize planted under optimal fertilization during the 2004/05 to 2007/08 growing seasons.

Weeping lovegrass

There was poor agreement between model prediction and measured values for weeping lovegrass high yield and LAI and all performance measures were far outside the acceptable ranges (Table 6, Figure 4). However, updating the soil water content in the model, using field measurements after each hay cut, improved model performance (Table 6, Figure 5).

Table 6. Performance measures from simulations with SWB-SCI after calibration for weeping lovegrass without and with updating soil water content after each hay cut using combined data collected during the 2004-2005 to 2007-2008 growing seasons.

Variables	**n**	**d**	**RMSE**	**MAE (%)**	**r^2**
Weeping lovegrass					
Without updating soil water content					
LAI	102	0.74	0.83	38	0.85
Aboveground biomass	102	0.51	1.97	37	0.74
Soil water content updated after every hay cut					
LAI	102	0.92	0.43	22	0.95
Aboveground biomass	102	0.84	1.13	22	0.91

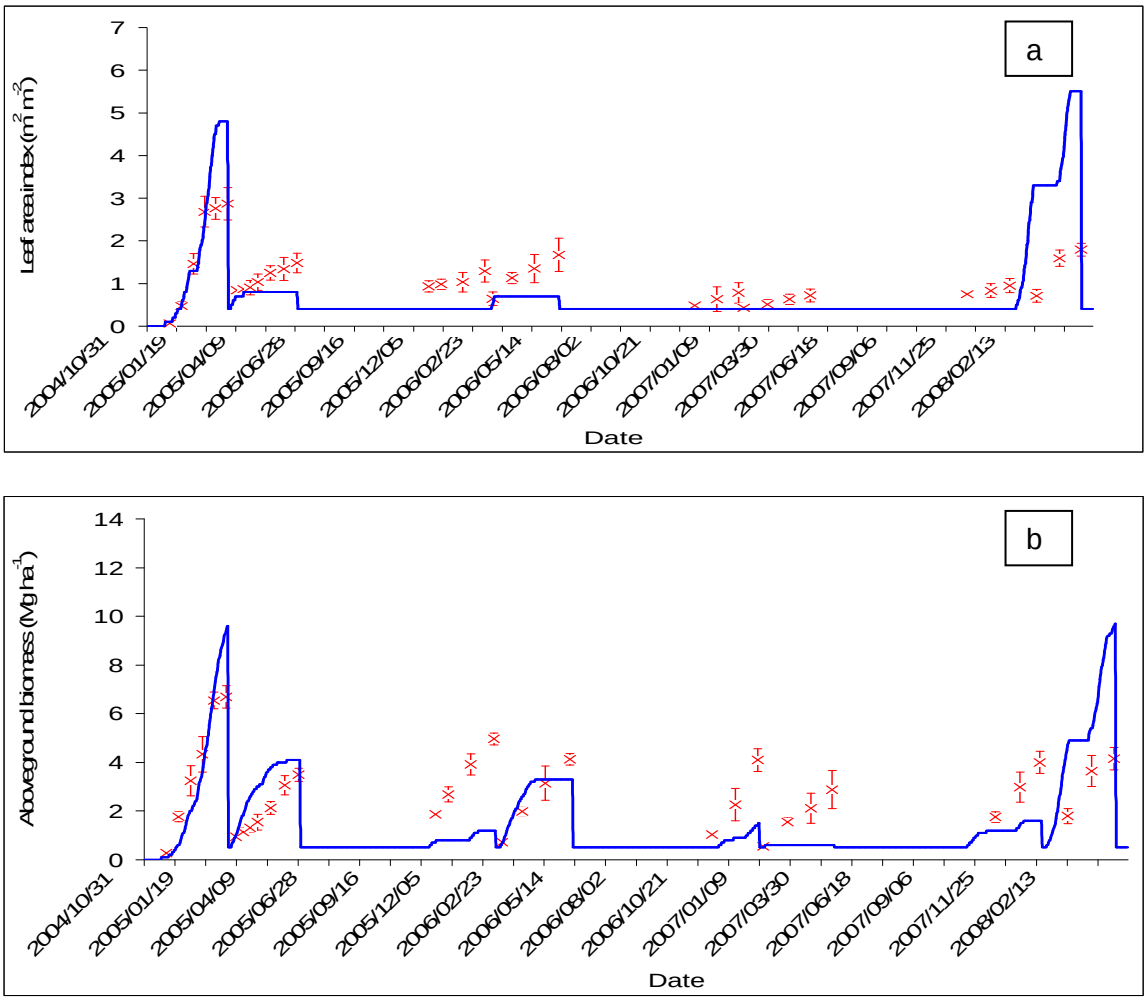

Figure 4. Simulated (solid lines) and measured values (symbols with standard deviation) of weeping lovegrass leaf area index (a) and aboveground biomass (b) during the 2004-2005 to 2007-2008 growing seasons (without updating soil water).

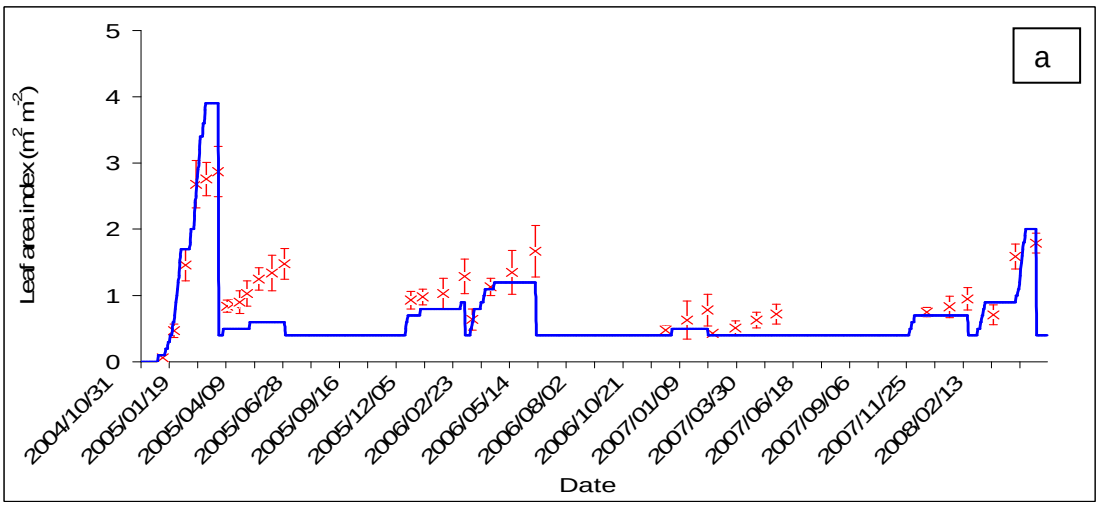

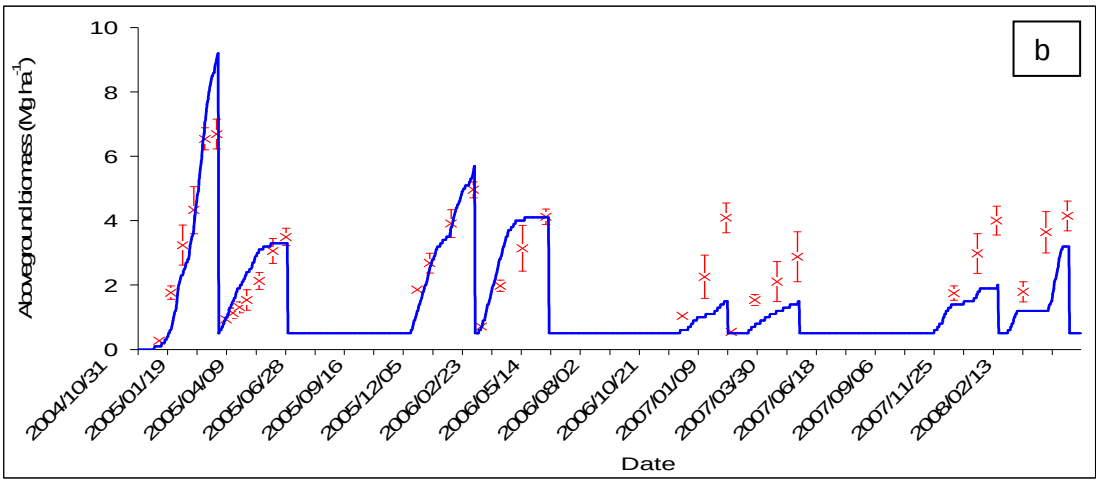

Figure 5. Simulated (solid lines) and measured values (symbols with standard deviation) of weeping lovegrass leaf area index (a) and aboveground biomass (b) during the 2004/05 to 2007/08 growing seasons (soil water content updated after every hay cut).

STICS crop model

Model calibration

STICS was run with a similar set of crop parameters as used to parameterize SWB-SCI. These parameters include: optimum temperature, minimum and maximum temperatures below which growth and development stop, thermal time requirements at various growth stages, and maximum crop height. Measured parameters required by STICS but not used by SWB-SCI or used as a seasonal average by SWB-SCI are presented in Table 7. Other parameters which were not measured were taken from the default values in STICS for the maize (cultivar DK250) and weeping lovegrass (cultivar Grass).

Table 7. Measured crop parameters used in STICS for medium season maize cultivar (PAN6966) and weeping love grass.

Parameter	Unit	Value		Source
		Maize	Weeping lovegrass	
Cumulative thermal time between the stages LEV (emergence) and AMF (maximum acceleration of leaf growth, end of juvenile phase)	degree days	200	116	Measured
Cumulative thermal time between the stages AMF (maximum acceleration of leaf growth, end of juvenile phase) and LAX (maximum leaf area index, end of leaf growth)	Degree days	700	6000 (default)	Measured (maize)
Cumulative thermal time between the stages LEV (emergence) and DRP (onset of filling of harvested organs)	degree days	1150	1000 (default)	Measured

Cumulative thermal time between FLO (flowering) and DRP (onset of filling of harvested organs)	degree days	150	100	Measured
Maximum grain weight (at 0% of water content)	g	0.313	0.01	Measured
Maximum SLA (specific leaf area) of green leaves	$cm^2\ g^{-1}$	250	70	Measured
Minimum SLA (specific leaf area) of green leaves	$cm^2\ g^{-1}$	80	50	Measured

STICS was calibrated using data collected from an irrigated inorganic fertilizer treatment for maize and dryland for weeping love grass. The main reason why we did not use the organic fertilizer treatments, which were used to calibrate and validate SWB-SCI, was to avoid any confounding errors that could occur due to improper parameterization of the organic material in STICS that could affect the availability of N for crop uptake.

A dataset containing field measurements of total aboveground biomass (t ha^{-1}) and leaf area index ($m^2\ m^{-2}$) dynamics as well as grain yield (t ha^{-1}) were used to test the success of model calibration.

Generally, the model was calibrated successfully for weeping love grass aboveground biomass and LAI (Figure 6a, b), because the performance measures were all within the ranges prescribed by De Jager *et al.* (1994) (Table 8).

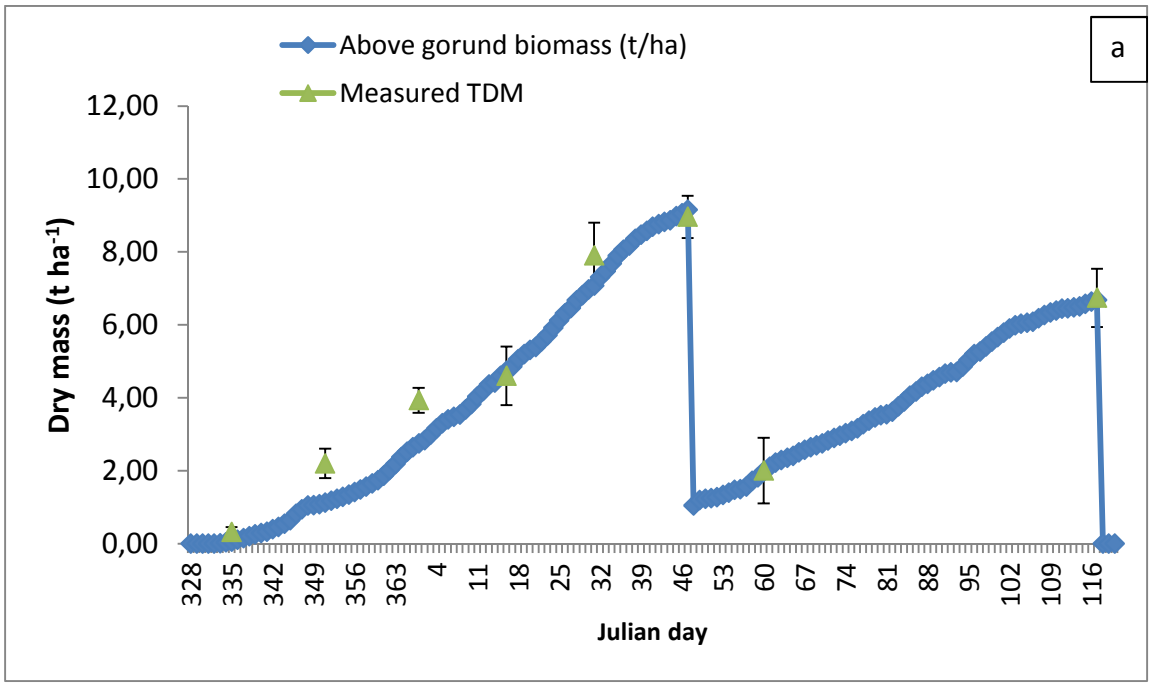

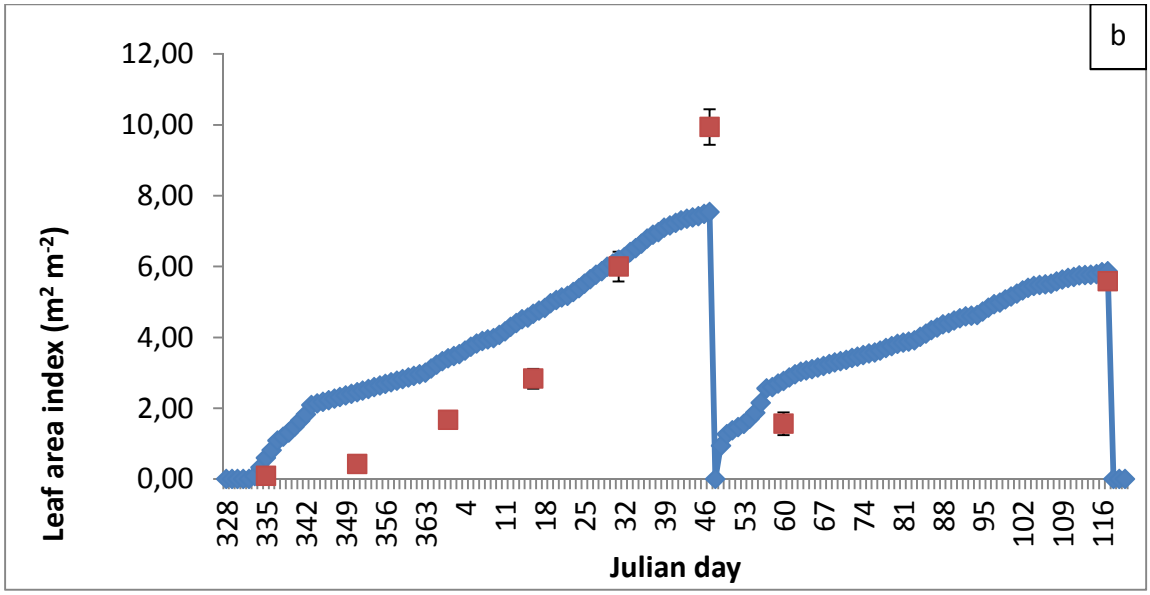

Figure 6. Simulated (solid lines) and measured values (symbols with standard deviation) for weeping lovegrass hay yield (a), and weeping lovegrass leaf area index (b).

Table 8. Performance measures from simulations obtained after STICS calibration for weeping lovegrass during the 2004-2005 growing season.

Variable	n	d	RMSE	MAE (%)	r^2
LAI	8	0.96	0.69	10.23	0.986
Aboveground biomass	8	0.82	1.51	35.06	0.928

Unlike weeping lovegrass, model calibration for maize was not satisfactory especially for LAI and grain yield (Figure 7a, b) because all the statistical parameters were outside the ranges prescribed by De Jager *et al.* (1994) (Table 9). The coefficient of correlation for aboveground biomass was, however, surprisingly high (93%). The main cause for the low coefficient of determination and relatively higher mean absolute error of the aboveground biomass production was mainly due to model underestimation during the vegetative till the beginning of the flowering stages. Similarly, the poor coefficient of correlation and determination as well as high mean absolute errors of the LAI were mainly due to model underestimation during the vegetative until beginning of flowering as well as model overestimation of LAI during the late flowering and grain filling stages. There is, however, a potential to improve the accuracy through parameter optimization.

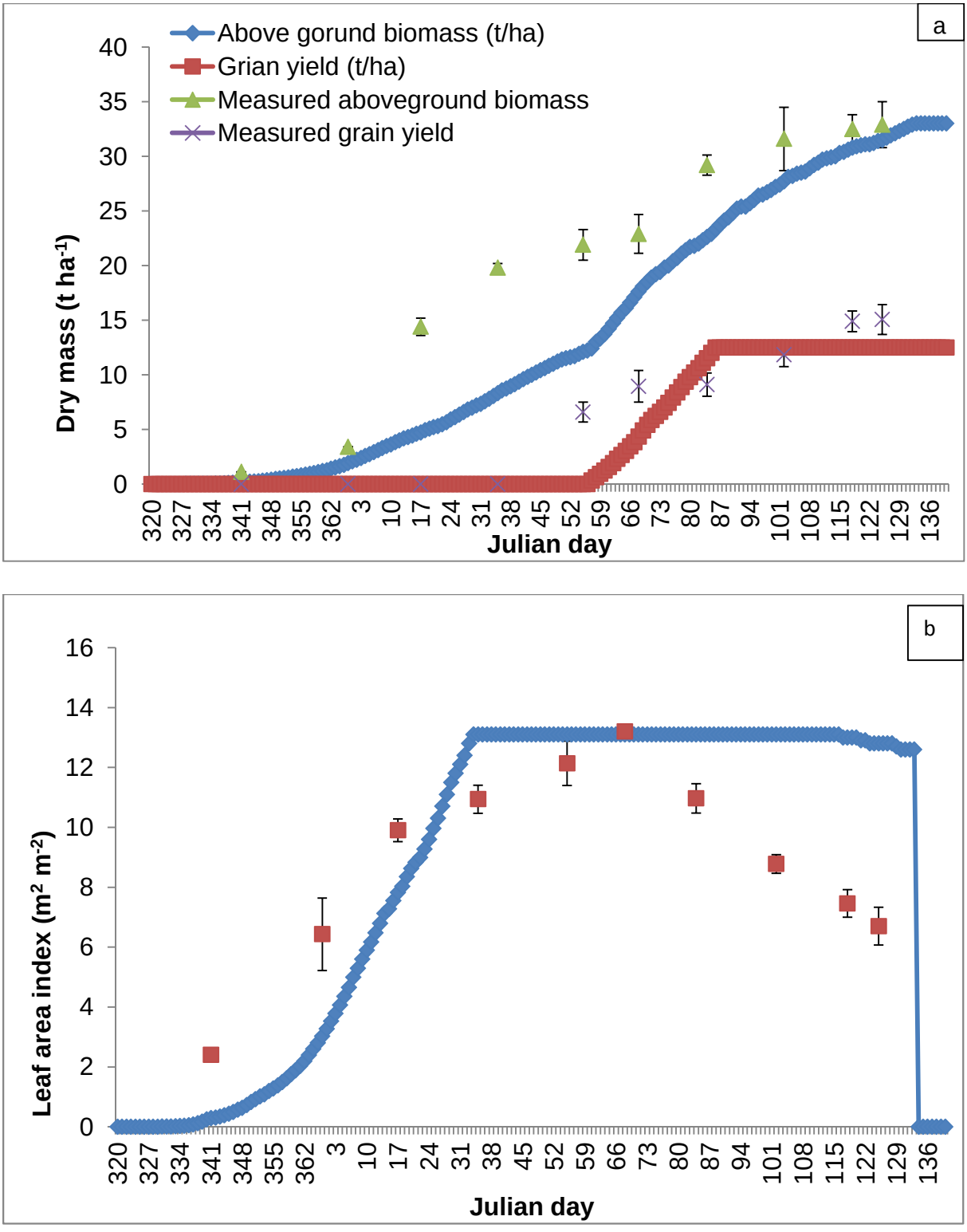

Figure 7. Simulated (solid lines) and measured values (symbols with standard deviation) for maize aboveground biomass (TDM) and grain yield (a) and maize leaf area index (b).

Table 9. Performance measures obtained from simulations with STICS after calibration for maize during the 2004-2005 growing season.

Variable	n	d	RMSE	MAE (%)	r^2
LAI	10	0.15	3.61	32.51	0.734
Aboveground biomass	10	0.68	6.81	24.96	0.943
Grain	6	0.12	3.15	0.21	0.65

Model corroboration

Model corroboration was conducted using variables from independent data sets collected during the 2005-2006 for weeping lovegrass and 2006-2007 growing season for maize. The variables used to evaluate the accuracy of the model were LAI, aboveground biomass and grain (agronomic crops) yield. Due to few measurement points, both aboveground biomass and grain yield for maize were combined for statistical evaluation of model accuracy.

Maize

The model predicted both aboveground biomass and grain yield with acceptable accuracy (Figure 8) for all the statistical parameters were within the prescribed ranges of accuracy (Table 10). This is despite the model's poor performance during calibration. Although it was not possible to conduct statistical evaluation of LAI because of very few measurement points (2), those two measurements were quite close to the model predicted values (Figure 8b).

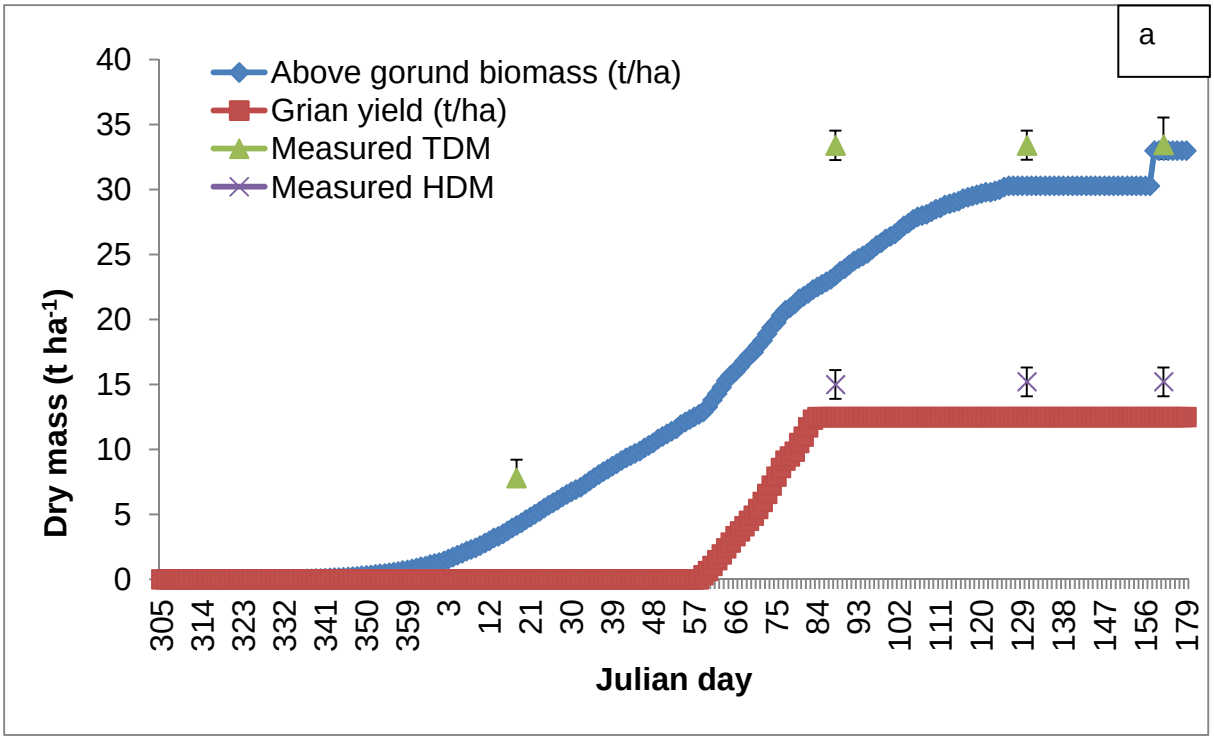

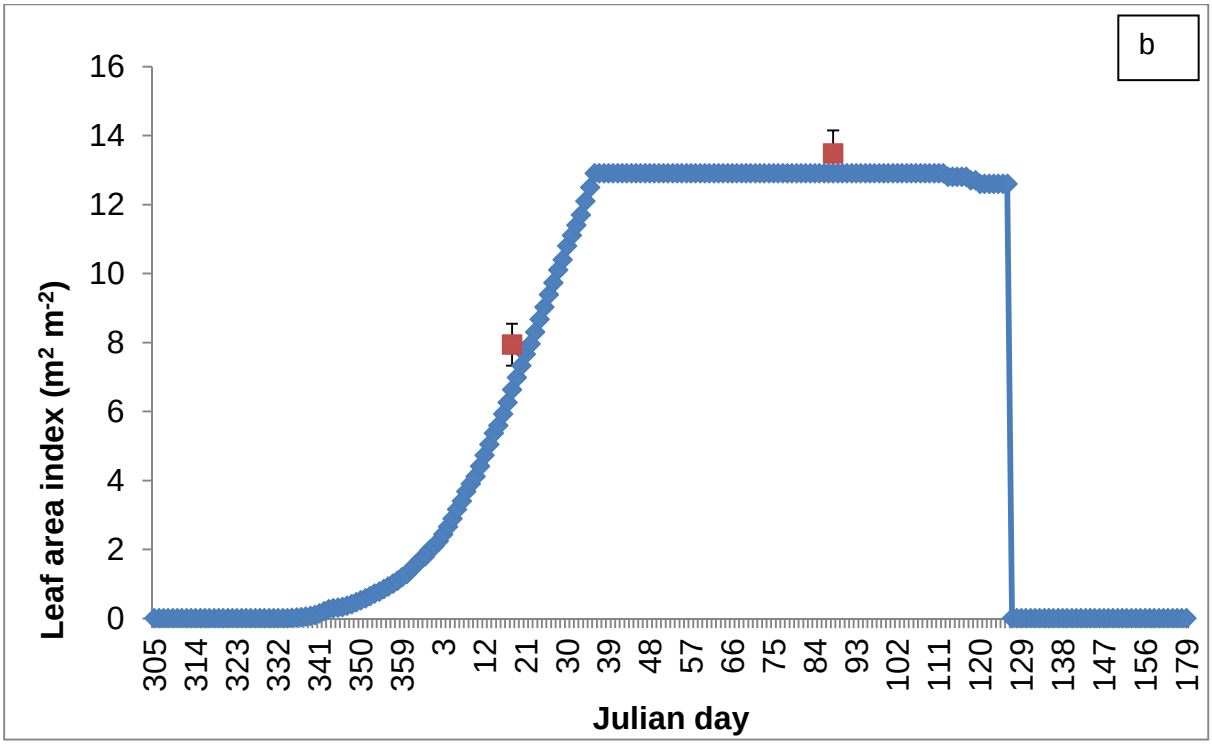

Figure 8. Simulated (solid lines) and measured values (symbols) of aboveground biomass (blue line) and grain yield (red line) (a) and leaf area index (b) for maize.

Table 10. Performance measures of STICS corroboration for dryland well fertilized maize (aboveground biomass and grain yield were combined together).

Variables	n	d	RMSE	MAE (%)	r^2
Aboveground biomass and grain	7	0.82	4.53	16.35	0.963

Weeping lovegrass

The model predicted weeping lovegrass aboveground biomass with high accuracy (Figure 9) having all the statistical parameters within the prescribed accuracy ranges (Table 11). There was, however, poor agreement between model prediction and measured values for weeping lovegrass leaf area index and all performance measures were far outside the acceptable ranges (Table 11, Figure 9b). The model overestimated LAI during most of the growing season.

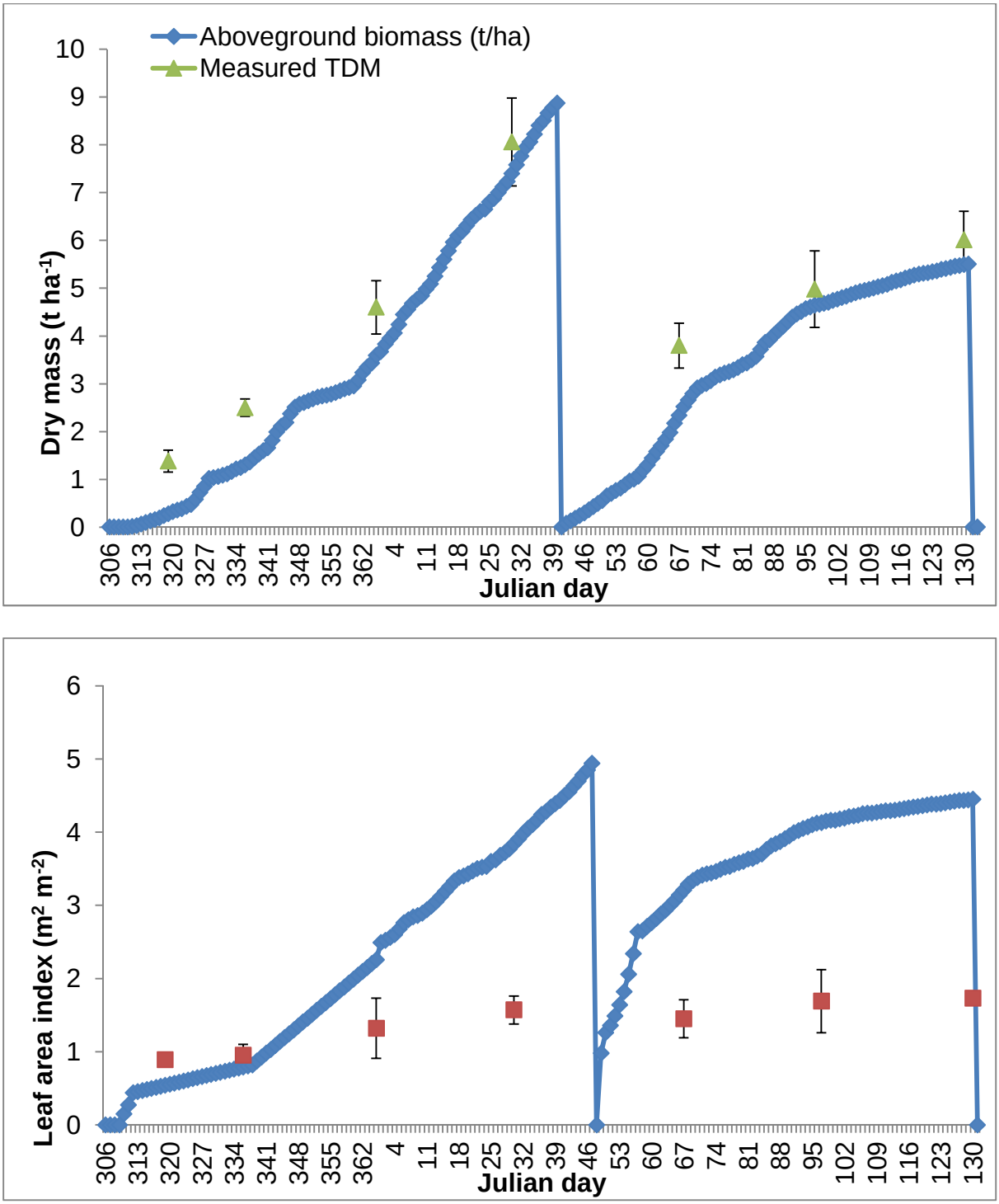

Figure 11. Simulated (solid lines) and measured values (symbols with standard deviation) of weeping lovegrass aboveground biomass (a) and leaf area index (b).

Table 9. Performance measures of STICS corroboration for weeping lovegrass.

Variables	n	d	RMSE	MAE (%)	r^2
Aboveground biomass	7	0.85	1.05	20.10	0.99
LAI	7	-0.12	1.21	392.06	0.78

Conclusions

Both SWB-SCI and STICS were calibrated and validated for maize and weeping lovegrass under South African climatic conditions. The calibration was successful for both models, except for STICS whose simulation for maize was not entirely satisfactory. Both models were tested against independent datasets and predicted the selected variables of interest for maize with acceptable accuracy. The predictive capability of both models for weeping lovegrass production was, however, relatively unsatisfactory, but not a complete failure. Therefore, both models can be used as reasoning support tools with caution especially when simulating perennial pastures in the tropics. It is also important to be cautious when using these models to simulate row crops such as maize whose biomass production of a specific cultivar per unit area could change due to a change in planting density or raw spacing, which is not accommodated in both models.

7. G-Range model: summary of activities

G-Range is a global model that simulates generalized changes in rangelands through time, created with support from the International Livestock Research Institute. Spatial data and a set of parameters that control plant growth and other ecological attributes in landscape units combine with computer code to represent ecological process such as soil nutrient and water dynamics, vegetation growth, fire, and wild and domestic animal offtake. The model is spatial, with areas of the world divided into square cells. Those cells that are rangelands have ecosystem dynamics simulated. A graphical user interface allows users to explore model output.

The G-Range application captures main primary production and its dynamics. It is of moderate complexity, and of a nature that a user may learn its use in a week or less. A monthly time step is used to simulate herbaceous plants, shrubs, and trees, and those plant types can change in their covers within each landscape cell through simulated time. The model represents all rangelands within a single computer process, which simplifies the logistics involved in analyses. Simulations may span a few to thousands of years.

Our efforts this year have been to establish a robust parameter set based on information from the literature, published spatial surfaces, and our experience. As part of this, we conducted a full sensitivity analysis.

To guide creation of a baseline simulation we required some data that would be deemed 'truth'. These data were used to compare to output from G-Range. The intent of these comparisons was not to yield a final parameter set that would represent well all areas within 15 biomes forever after. Instead, it was to allow adjustment of parameters to change G-Range output from essentially uncontrolled to something more in agreement with reality. In-so-far as that was the goal, only cursory effort was put into determining the validity of what is here deemed 'truth'; we proceeded knowing that comparing results to published or vetted data would be helpful. That includes simulated output from the Century model. That model has been vetted many times and gridded summaries of simulations are suitable for comparison with G-Range output.

We adopted a spatially explicit means of comparing global responses from G-Range to various responses. Simulations started in 1957 and continued for 50 years, to 2006. Where year-specific data were available, data from 2006 were used. For some spatial data, specific years were not available, and so recent general responses were used. In this baseline simulation, fire was not incorporated and fertilization has not been included. More than 120 simulations were conducted while parameters were adjusted and the fit of the model output was improved. During that effort we began to learn about the ways in which parameters of G-Range influence model output. Most often responses were in the direction expected based on the processes the parameter informs, but sometimes the results were surprising. A subset of those surprises led to modify the G-Range code. Ultimately, modifications seemed to be no longer improving the fit of the model, and the parameter set was judged suitable for the subsequent sensitivity analyses.

Approach

Annual net primary production (NPP) is a key ecosystem process to be validated in ecosystem models, as it comprises annual inputs of energy to ecosystems via photosynthesis. Aboveground production (ANPP) is, moreover, an estimate of forage

production in rangelands, while belowground production (BNPP) significantly regulates soil C levels. Field production data on ANPP and BNPP (in g m^{-2}) were compiled from Oak Ridge National Laboratory database (Scurlock and Olson 2002) and the Long-Term Ecosystem Research network (Abrams *et al.*, 1986; Briggs *et al.*, 1989, Knapp *et al.*, 1998; Huenneke *et al.*, 2002, Heisler and Knapp, 2008; Muldavin *et al.*, 2008). A total of 28 independent studies in 25 sites represented global variation in biomes that include rangelands, varying widely in mean annual precipitation (200 to 1300 mm) and temperature (-4 to 29 °C).

ANPP was calculated as peak standing crop, a measure with low uncertainty (Lauenroth *et al.*, 2006). BNPP was calculated as the mean of high (likely overestimates) and low (likely underestimates) of measures of root biomass production in each site. Minirhizotron, stable isotope, and root in growth estimates were utilized where available (Milchunas, 2009); otherwise maximum and maximum-minimum root biomass were used, respectively, as high and low estimates of root production with known directional biases and low uncertainty (Lauenroth *et al.*, 2006). G-Range parameters divided among biomes as defined in the SAGE map (Ramankutty and Foley, 1999) were tuned to improve mean biome-level absolute difference and root mean squared error (RMSE) between modelled and observed ANPP and BNPP.

Results

Beginning from the baseline parameter set for the beta version of G-Range, sensitivity analyses and parameter adjustment realized substantial improvement in model fit. Two parameter sets representing this improvement (Figure 1) are presented here: ‘Set 1’ was developed using site-scale analyses, by tuning several parameters related to biomass production and allocation above- and belowground; and ‘Set 2’ was developed from global analyses, applied here at site scales.

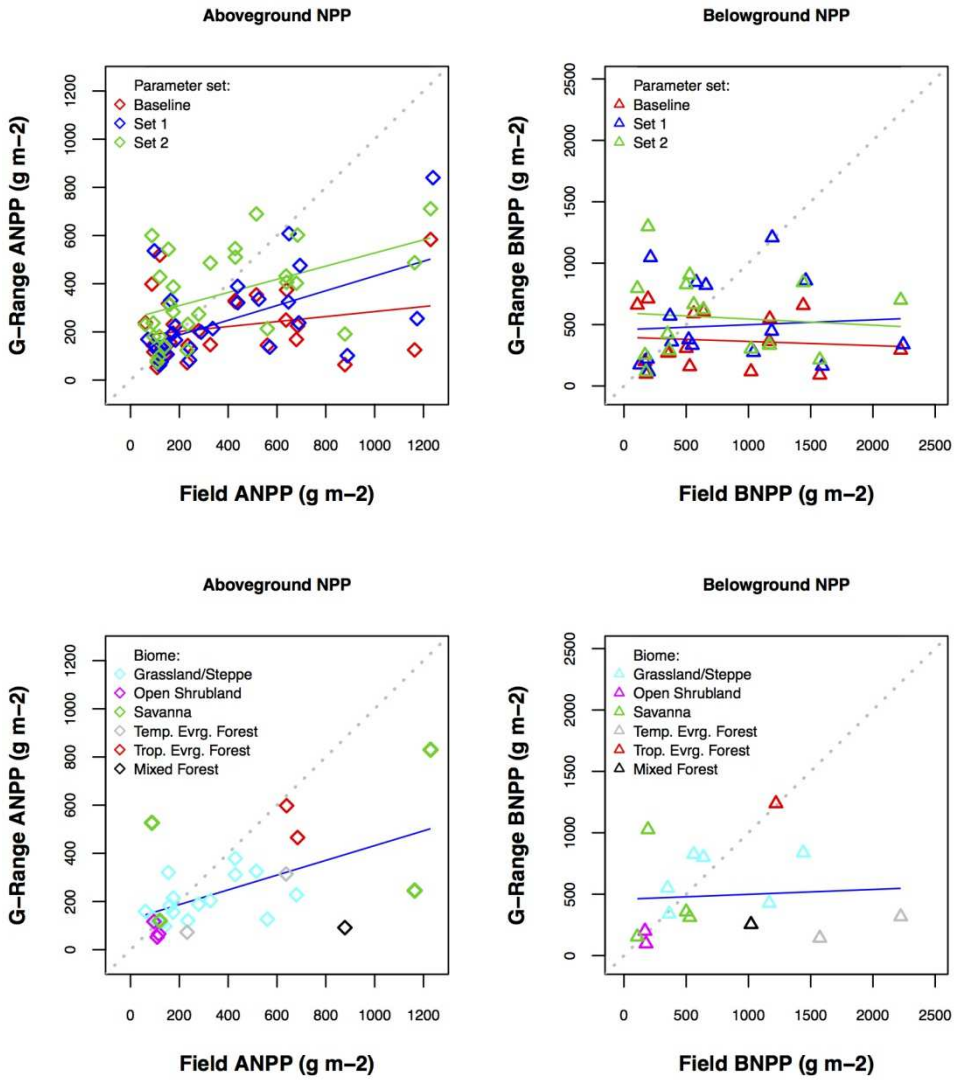

Figure 1. G-Range model fit assessed on the basis of field aboveground (ANPP) and belowground (BNPP) production estimates, among sites and biomes for 3 parameterizations (upper panels), and among sites within biomes for parameter 'Set 1' (lower panels).

Mean values among sites in all biomes for absolute difference and root mean squared error (RMSE) between modelled and observed ANPP improved, respectively, from -156.2 to -18.8, and from 352.0 to 282.6 using parameter Set 2. Absolute difference and RMSE for BNPP improved from -390.4 to -203.9, and from 756.6 to 710.7 using Set 1. Linear regression R^2 values among sites in all biomes increased from 0.026 for the baseline parameterization to 0.274 (Set 1) and 0.204 (Set 2) for ANPP (Figure 1). Typical rangeland biomes exhibited better model fit, including 'Grassland/Steppe' (minimum absolute difference for Set 1 or Set 2 = -80.4 for ANPP, -123.1 for BNPP), 'Savanna' (-219.5, 130.1), and 'Open Shrubland' (10.1, 11.2), *i.e.*, semi-desert, as did 'Tropical Evergreen Forest' (-130.1, 17.4), than the somewhat less extensive rangeland biomes 'Temperate Evergreen Forest' (-156.6, -1441.6) and 'Mixed Evergreen/Deciduous Forest' (-687.0, -718.6).

8. References

Abrams, M.D., Knapp, A.K., Hulbert, L.C., 1986. A 10-year record of aboveground biomass in a Kansas tallgrass prairie - Effects of fire and topographic position. Am. J. Bot., 73, 1509-1515.

Annandale, J.G., Benadé, N., Jovanovic, N.Z., Steyn, J.M., Du Sautoy, N., 1999. Facilitating irrigation scheduling by means of the Soil Water Balance model. Water Research Commission Report No. 753/1/99, Pretoria, South Africa.

Araujo, L.C., 2011. Modelos matemáticos para estimar a sazonalidade de produção em pastagem de Panicum maximum cv. Mombaça em regiões do Estado de São Paulo. PhD Thesis. University of São Paulo, Piracicaba, São Paulo, Brazil, 87 p. (in Brazilian Portuguese)

Barnard, R.O., Rethman, N.F.G., Annandale, J.G., Mentz, W., Jovanovic, N.Z., 1998. The screening of crop, pasture and wetland species for tolerance of polluted water originating in coal mines. Water Research Commission Report No. 582/1/98, Pretoria, South Africa.

Ben Touhami, H., 2014. Calibration Bayésienne d'un modèle d'étude d'écosystème prairial : outils et applications à l'échelle de l'Europe. PhD Thesis, Blaise Pascal University, Clermont-Ferrand (in French).

Ben Touhami, H., Bellocchi, G., 2014. Bayesian calibration of the Pasture Simulation model (PaSim) to simulate emissions from long-term grassland sites: a European perspective. Livestock, Climate Change and Food Security Conference, May 19-20, Madrid, Spain, ANIMALCHANGE2014/8.

Ben Touhami, H., Lardy, R., Barra, V., Bellocchi, G., 2013a. Screening parameters in the Pasture Simulation model using the Morris method. Ecol. Modell., 266, 42–57.

Ben Touhami, H., Lardy, R., Bellocchi, G., 2013b. Tools for model evaluation and parameterization. AnimalChange project deliverable D15.2.

Béziat, P., Ceschia, E., Dedieu, G., 2009. Carbon balance of a three crop succession over two cropland sites in South West France. Agr. Forest Meteorol., 149, 1628-1645.

Boé, J., Terray, L., Habets, F., Martin, E., 2006. A simple statistical-dynamical downscaling scheme based on weather types and conditional resampling. J. Geophys. Res., 111, D23106.

Briggs, J.M., Seastedt, T.R., Gibson, D.J., 1989. Comparative analysis of temporal and spatial variability in above-ground production in a deciduous forest and prairie. Holarct. Ecol., 12, 130-136.

Brisson, N., Gary, C., Justes, E., Roche, R., Mary, B., Ripoche, D., Zimmer, D., Sierra, J., Bertuzzi, P., Burger, P., Bussiere, F., Cabidoche, Y. M., Cellier, P., Debaeke, P., Gaudillere, J. P., Henault, C., Maraux, F., Seguin, B., Sinoquet, H., 2003. An overview of the crop model STICS. Eur. J. Agron., 18, 309-332.

Broomhead, D.S., King, G.P., 1986. Extracting qualitative dynamics from experimental data. Physica D, 20, 217–236.

Bull, 2014. Bull, Architect for an Open World™. Les Clayes-sous-Bois. <http://www.bull.com> (accessed 31.01.14).

Bunting, E.S., 1976. Accumulated temperature and maize development in England. J. Agric. Sci., 87, 577-583.

Büttner, G., Feranec, J., Jaffrain, G., Mari, L., Maucha, G., Soukup, T., 2004. The CORINE Land Cover 2000 Project. EARSeL eProceedings, 3, 331-346.

Carvalhais, N., Reichstein, M., Seixas, J., Collatz, G.J., Santos Pereira, J., Berbigier, P., Carrara, A., Granier, A., Montagnani, L., Papale, D., Rambal, S., Sanz, M.J., Valentini, R., 2008. Implications of the carbon cycle steady state assumption for biogeochemical modeling performance and inverse parameter retrieval. Global Biogeochem. Cy., 22:GB2007.

CCRT, 2014. Titane. Centre de calcul, recherche et technologie, Bruyères-le-Châtel. <http://www-ccrt.cea.fr/fr/moyen_de_calcul/titane.htm> (accessed 31.01.14, in French).

Ciais, P., Reichstein, M., Viovy, N., Granier, A., Ogee, J., Allard, V.,Aubinet, M., Buchmann, N., Bernhofer, C., Carrara, A., Chevallier, F., De Noblet, N., Friend, A. D., Friedlingstein, P., Grunwald, T., Heinesch, B., Keronen, P., Knohl, A., Krinner, G., Loustau, D., Manca, G., Matteucci, G., Miglietta, F., Ourcival, J. M., Papale, D., Pilegaard, K., Rambal, S., Seufert, G., Soussana, J. F., Sanz, M. J., Schulze, E. D., Vesala, T., Valentini, R., 2005. Europewide reduction in primary productivity caused by the heat and drought in 2003, Nature, 437, 529–533.

Cox, J.R., Martin-R.M.H., Ibarra-F, F.A., Fourie, J.H., Rethman, N.F.G., Wilcox, D.G., 1988. The influence of climate and soils on the distribution of four African grasses. Journal of Range Management, 41, 127-139.

Dalrymple, R.L., 1976. Weeping lovegrass management. Ardmore, OK: Noble Foundation, Agriculture Division, 19 p.

DataONE, 2014. Panoply data viewer. Data Observation Network for Earth, Albuquerque, NM. <http://www.dataone.org/software-tools/panoply-data-viewer> (accessed 31.01.14).

De Jager, J.M., 1994. Accuracy of vegetation evaporation ratio formulae for estimating final wheat yield. Water SA, 20, 307-314.

Dolman, A.J., Tolk, L., Ronda, R., Noilhan, J., Sarrat, C., Brut, A., Piguet, B., 2006. The CarboEurope regional experiment strategy. Bull. Amer. Meteor. Soc., 87, 1367–1379.

Ducoudre, N.I., Laval, K., Perrier, A., 1993. Sechiba, a new set of parameterizations of the hydrologic exchanges at the land atmosphere interface within the lmd atmospheric general-circulation model. J. Climate, 6, 248-273.

Elsner, J.B., Tsonis, A.A., 1996. Singular spectrum analysis: a new tool in time series analysis, Plenum, New York, 164 p.

Eurostat, 2007. Regions in the European Union – Nomenclature of territorial units for statistics – NUTS 2006 /EU-27.

Gabrielle, B., Laville, P., Duval, O., Nicoullaud, B., Germon, J.C., Hénault, C., 2006. Process-based modeling of nitrous oxide emissions from wheat-cropped soils at the subregional scale. Global Biogeochem. Cy., 20, GB4018.

Ghil, M., Allen, M.R., Dettinger, M.D., Ide, K., Kondrashov, D., Mann, M.E., Robertson, A.W., Saunders, A., Tian, Y., Varadi, F., Yiou, P., 2002. Advanced spectral methods for climatic time series. Rev. Geophys., 40, 1003.

Golyandina, N., Nekrutkin, V., Zhigljavsky, A., 2001. Analysis of time series structure: SSA and related techniques, Monogr. Stat. Appl. Probab., vol. 90, CRC Press, Boca Raton, p. 305.

Graux, A.-I., 2011. Modelling climate change impacts on grassland ecosystems. Ways to adapt forage systems. PhD Thesis, Blaise Pascal University, Clermont-Ferrand.

Graux, A.-I., Bellocchi, G., Lardy, R., Soussana, J.-F., 2013. Ensemble modelling of climate change risks and opportunities for managed grasslands in France. Agr. Forest Meteorol., 170, 114-131.

Graux, A.I., Gaurut, M., Agabriel, J., Baumont, R., Delagarde, R., Delaby, L., Soussana, J.F., 2011. Development of the Pasture Simulation Model for assessing livestock production under climate change. Agr. Ecosyst. Environ., 144, 69–91.

Graux, A.-I., Lardy, R., Bellocchi, G., Soussana, J.-F., 2012. Global warming potential of French grassland-based dairy livestock systems under climate change. Reg. Environ. Change, 12, 751-763.

Gulden, L.E., Rosero, E., Yang, Z.-L., Wagener, T., Niu, G.-Y., 2008. Model performance, model robustness, and model fitness scores: a new method for identifying good land-surface models, Geophys. Res. Lett., 35, L11404.

Heisler, J.L., Knapp, A.K., 2008. Temporal coherence of aboveground net primary productivity in mesic grasslands. Ecography, 31, 408-416.

Hensley, M., van den Berg, W.J., Anderson, J.J. Oberholzer, L.J. Du Toit, M.S., Berry, W., de Jager J.M., 1994. Modelling the water balance of benchmark ecotopes. Water Research Commisssion Progress Rep., Pretoria, South Africa.

Huenneke, L.F., Anderson, J.P., Remmenga, M., Schlesinger, W.H., 2002. Desertification alters patterns of aboveground net primary production in Chihuahuan ecosystems. Global Change Biol., 8, 247-264.

IPCC, 2000. A2 Storyline and Scenario Family. In: Nakičenovič, N., Swart, R., (Eds.), Summary for Policymakers, Intergovernmental Panel of Climate Change, Geneva. <http://www.ipcc.ch/ipccreports/sres/emission/index.php?idp=94> (accessed 31.01.14).

IPCC, 2006. IPCC guidelines for national greenhouse gas inventories, prepared by the National Greenhouse Gas Inventories Programme, Eggleston, H.S., Buendia, L., Miwa, K., Ngara, T., Tanabe, K. (eds). IGES, Japan.

IPSL, 2014. ORCHIDEE, France Global Land Surface Model. Pierre-Simon Laplace Institute, Guyancourt. <http://orchidee.ipsl.jussieu.fr> (accessed 30.01.14).

IUCN/UNEP/WWF, 1991. Caring for the Earth. A strategy for sustainable living. IUCN/UNEP/WWF, Gland, Switzerland.

Johnson IR (2012). PlantMod: exploring the physiology of plant canopies. IMJ Software, Melbourne, Vic, Australia (available at: http://www.imj.com.au/software/plantmod).

Johnson, I.R., Chapman, D.F., Snow, V.O., Eckard, R.J., Parsons, A.J., Lambert, M.G., Cullen, B.R., 2008. DairyMod and EcoMod: biophysical pastoral simulation models for Australia and New Zealand. Aust. J. Exp. Agric., 48, 621-631.

Keeling, P.L., Greaves, J.A., 1990. Effects of temperature stresses on corn-opportunities for breeding and biotechnology. Proceedings of the 45th Annual Corn and Sorghum Research Conference, 29-42.

Kenny, G.J., Harrison, P.A., 1992. Thermal and moisture limits of grain maize in Europe: model testing and sensitivity to climate change. Clim. Res., 2, 113-129.

Klumpp, K., Tallec, T., Guix, N., Soussana, J.-F., 2011. Long-term impacts of agricultural practices and climatic variability on carbon storage in a permanent pasture. Global Change Biol., 17, 3534-3545.

Knapp, A.K., Briggs, J.M., Hartnett, D.C., Collins, S.L., 1998. Grassland dynamics: long-term ecological research in tallgrass prairie. Oxford University Press, New York, NY.

Knapp, A.K., Briggs, J.M., Koelliker, J.K., 2001. Frequency and extent of water limitation to primary production in a mesic temperate grassland. Ecosystems, 4, 19–28.

Krinner, G., Viovy, N., de Noblet-Ducoudre, N., Ogee, J., Polcher, J., Friedlingstein, P., Ciais, P., Sitch, S., Prentice, I.C., 2005. A dynamic global vegetation model for studies of the coupled tmosphere-biosphere system. Global. Biogeochem. Cy., 19, GB1015.

Lara, M.A.S., 2011. Respostas morfofisiológicas de genótipos de Brachiaria spp sob duas intensidades de desfolhação e modelagem da produção de forragem em função das variações estacionais da temperatura e fotoperíodo: adaptação do modelo CROPGRO. PhD Thesis, University of São Paulo, Piracicaba, São Paulo, Brazil, 212 p. (in Brazilian Portuguese)

Lardy, R., Bellocchi, G., Soussana, J.-F., 2011. A new method to determine soil organic carbon equilibrium. Environ. Modell. Softw., 26, 1759-1763.

Lauenroth, W.K., Wade, A.A, Williamson, M.A., Ross, B.E., Kumar, S., Cariveau, D.P., 2006 Uncertainty in calculations of net primary production for grasslands. Ecosystems, 9, 843-851.

Le Bauer, D.S., Treseder, K.K., 2008. Nitrogen limitation of net primary productivity in terrestrial ecosystems is globally distributed. Ecology, 89, 371–379.

Legates, D.R., McCabe, G.J., Jr., 1999. Evaluating the use of “goodness-of-fit” measures in hydrologic and hydroclimatic model validation. Water Resour. Res., 35, 233–241.

Le Houerou, H.N., Bingham, R.L., Skerbek, W., 1988. Relationship between the variability of primary production and the variability of annual precipitation in world arid lands. J. Arid Environ., 15, 1- 8.

Mahecha, M.D., Reichstein, M., Carvalhais, N., Lasslop, G., Lange, H., Seneviratne, S.I., Vargas, R., Ammann, C., Arain, M.A., Cescatti, A., Janssens, I.A., Migliavacca, M., Montagnani, L., Richardson, A.D., 2010. Global convergence in the temperature sensitivity of respiration at ecosystem level. Science, 329, 838–840.

McMaster, G.S., Wilhelm, W.W., 1997. Growing degree-days: one equation, two interpretations. Agr. Forest Meteorol., 87, 291-300.

Milchunas, D.G., 2009. Estimating root production: comparison of 11 methods in shortgrass steppe and review of biases. Ecosystems, 12, 1381-1402.

Moffat, A.M., Papale, D., Reichstein, M., Holinger, D.Y., Richardson, A.D., Barr, A.G., Beckstein, C., Braswell, B.H., Churkina, G., Desai, A.R., Falge, E., Gove, J.H., Heinmann, M., Hui, D.F., Jarvis, A.J., Kattge, J., Noormets, A., Stauch, V.J., 2007. Comprehensive comparison of gap-filling techniques for eddy covariance net carbon fluxes. Agr. Forest Meteorol., 147, 209–232.

Muldavin, E.H., Moore, D.I., Collins, S.L., Wetherill, K.R., Lightfoot, D.C., 2008. Aboveground net primary production dynamics in a northern Chihuahuan Desert ecosystem. Oecologia, 155, 123-132.

Nippert, J.B., Knapp, A.K., Briggs, J.M., 2006, Intra-annual rainfall variability and grassland productivity: can the past predict the future? Plant Ecology, 184, 65–74.

Olesen, J.E., Carter, T.R., Díaz-Ambrona, C.H. Fronzek, S., Heidmann, T., Hickler, T., Holt, T., Minguez, M.I., Morales, P., Palutikof, J., Quemada, M., Ruiz-Ramos, M., Rubæk, G., Sau, F., Smith, B., Sykes, M., 2007. Uncertainties in projected impacts of climate change on European agriculture and terrestrial ecosystems based on scenarios from regional climate models. Climatic Change, 81, 123-143.

Papale, D, Reichstein, M., Aubinet, M., Canfora, E., Bernhofer, C., Kutsch, W., Longdoz, B., Rambal, S., Valentini, R., Vesala, T., Yakir, D., 2006. Towards a standardized processing of Net Ecosystem Exchange measured with eddy covariance technique: algorithms and uncertainty estimation. Biogeosciences, 3, 571-583.

Parton, W.J., 1988. Dynamic of C, N, S and P in grassland soils: a model. Biogeochemistry, 5, 109-131.

Peeters, A., 2009. Importance, evolution, environmental impact and future challenges of grasslands and grassland-based systems in Europe. Grassland Science, 55, 113–125.

Piao, S., Fang, J., Zhou, L., Tan, K., Tao, S., 2007. Changes in biomass carbon stocks in China's grasslands between 1982 and 1999. Global Biogeochem. Cy., 21, GB2002.

Ramankutty, N., Foley, J.A., 1999. Estimating historical changes in global land cover: Croplands from 1700 to 1992. Global Biogeochem. Cy., 13, 997-1027.

Reichstein, M., Falge, E., Baldocchi, D., Papale, D., Aubinet, M., Berbigier, P., Bernhofer, C., Buchmann, N., Gilmanov, T., Granier, A., Grunwald, T., Havrankova, K., Ilvesniemi, H., Janous, D., Knohl, A., Laurila, T., Lohila, A., Loustau, D., Matteucci, G., Meyers, T., Miglietta, F., Ourcival, J.-M., Pumpanen, J., Rambal, S., Rotenberg, E., Sanz, M., Tenhunen, J., Seufert, G., Vaccari, F., Vesala, T., Yakir, D., Valentini, R., 2005. On the separation of net

ecosystem exchange into assimilation and ecosystem respiration: review and improved algorithm. Global Change Biol., 11, 1424-1439.

Riedo, M., Grub, A., Rosset, M., Fuhrer, J., 1998. A pasture simulation model for dry matter production, and fluxes of carbon, nitrogen, water and energy. Ecol. Modell., 105, 141–183.

Riedo, M., Milford, C., Schmid, M., Sutton, M.A., 2002. Coupling soil-plant-atmosphere exchange of ammonia with ecosystem functioning in grasslands. Ecol. Modell., 158, 83–110.

Scurlock, J.M.O., Olson, R.J., 2002. Terrestrial net primary productivity - A brief history and a new worldwide database. Environ. Rev., 10, 91-109.

Shaw, R.H., 1983. Estimates of yield reduction in corn caused by water and temperature stress. In: Raper, D.C., Kramer, P.J. (eds.) Crop reactions to water and temperature stresses in humid temperate climates. Westview Press, Boulder, CO, 49-66.

Schmid, M., Neftel, A., Riedo, M., Fuhrer, J., 2001. Process-based modelling of nitrous oxide emissions from different nitrogen sources in mown grassland. Nutr. Cycl. Agroecosys., 60, 177–187.

Smit, H.J., Metzger M.J., Ewert, F., 2008. Spatial distribution of grassland productivity and land use in Europe. Agric. Syst., 98, 208–219.

Soussana, J.-F., Graux, A.-I., Tubiello, F.N., 2010. Improving the use of modelling for projections of climate change impacts on crops and pastures. J. Exp. Bot., 61, 2217-2228.

Tubiello, F.N., Soussana, J.-F., Howden, S.M., 2007. Crop and pasture responses to climate change. P. Natl. Acad. Sci. U.S.A., 104, 19686-19690.

UNIDATA (2014) Network Common Data Form (NetCDF). Unidata Program Center, University Corporation for Atmospheric Research, Boulder, CO. <http://www.unidata.ucar.edu/software/netcdf> (accessed 31.01.14).

Van Oijen, M., Thomson, A., 2010. Toward Bayesian uncertainty quantification for forestry models used in the United Kingdom Greenhouse Gas Inventory for land use, land use change, and forestry. Climatic Change, 103, 55-67.

Viovy, N., de Noblet, N., 1997. Coupling water and carbon cycle in the biosphere. Sci. Géol. Bull., 50, 109-121.

Vuichard, N., Ciais, P., Viovy, N., Calanca, P., Soussana, J.-F., 2007a. Estimating the greenhouse gas fluxes of European grasslands with a process-based model: 2. Simulations at the continental level. Global Biogeochem. Cy. 21, GB1005.

Vuichard, N., Soussana, J.-F., Ciais, P., Viovy, N., Ammann, C., Calanca, P., Clifton-Brown, J., Fuhrer, J., Jones, M., Martin, C., 2007b. Estimating the greenhouse gas fluxes of European grasslands with a process-based model: 1. Model evaluation from in situ measurements. Global Biogeochem. Cy. 21, GB1004.

Wallach, D., Buis, S., Lecharpentier, P., Bourges, J., Clastre, P., Launay, M., Bergez, J.-E., Guérif, M., Soudais, J., Justes, E. (2011) A package of parameter estimation methods and implementation for the STICS crop-soil model. Environ. Modell. Softw., 26, 1-9.

Weedon, G.P., Gomes, S., Viterbo, P., Österle, H. Adam, J.C., Bellouin, N., Boucher, O., Best, M., 2010. The WATCH forcing data 1958-2001: a meteorological forcing dataset for land surface and hydrological models. WATCH Technical Report 22, 41 p. (available at www.eu-watch.org/publications).

Weedon, G.P., Gomes, S., Viterbo, P., Shuttleworth, W.J., Blyth, E., Österle, H., Adam, J.C., Bellouin, O., and Best, M., in press, 2011. Creation of the WATCH forcing data and its use to assess global and regional reference crop evaporation over land during the twentieth century. J. Hydrometeor., 12, 823–848.

Willmott, C.J. (1982) Some comments on the evaluation of model performance. Bull. of Am. Meteorol. Soc., 64, 1309-1313.

Willmott, C.J., Ackleson, S.G., Davis, R.E., Feddema, J.J., Klink KM, Legates, D.R., O'Donnell, J., Rowe, C.M., 1985. Statistics for the evaluation of model performance. J. Geophys. Res., 90, 8995–9005.

Wint, G.R.W., Robinson, T.P., 2007. Gridded livestock of the world 2007. Food and Agriculture Organization of the United Nations (FAO), Rome, Italy, 131 p.

Wirsenius, S., 2000. Human use of land and organic materials: modeling the turnover of biomass in the global food system. Department of Physical Resource Theory, Chalmers University of Technology, Göteborg University, Göteborg, Sweden.

Wriedt, G., van der Velde, M., Aloe, A., Bouraoui, F., 2009, A European irrigation map for spatially distributed agricultural modeling. Agr. Water Manage., 96, 771–789.

Xia, J., Wan, S., 2008. Global response patterns of terrestrial plant species to nitrogen addition. New Phytol., 179, 428-439.